Ulm University
Institute of Molecular and Cellular Anatomy
Director: Prof. Dr. med. Stefan Britsch

Compensatory functions of the zinc-finger transcription factors Bcl11a and Bcl11b and their effects on neocortical development

Dissertation to obtain the doctoral degree of medicine (Dr. med.)
at the Faculty of Medicine, Ulm University

Simeon Gaessler
Stuttgart, Germany

2017

Present dean	Prof. Dr. T. Wirth
First correspondent	Prof. Dr. S. Britsch
Second correspondent	Prof. Dr. N. Golenhofen
Date of promotion	10.01.2019

Research of this medical thesis contributed to the following publication:

Wiegreffe, C., Feldmann, S., Gaessler, S., & Britsch, S. (2017) Time-Lapse Confocal Imaging of Migrating Neurons in Organotypic Slice Culture of Embryonic Mouse Brain using *in Utero* Electroporation. *JoVe (Journal of Visualized Experiments),* (152), e55886.

Table of contents

I List of abbreviations III
1.0 Introduction 1
1.1 Anatomy and development of the neocortex 1
1.2 Transcription factors 4
1.2.1 Bcl11a 4
1.2.2 Bcl11b 6
1.2.3 Deep-layer specific transcription factors 8
1.2.4 Upper-layer specific transcription factors 8
1.3 Aims of my thesis 9
2.0 Materials and Methods 11
2.1 Materials 11
2.2 Methods 16
2.2.1 Cre/loxP system 16
2.2.2 Gene-modified animals and mating system 17
2.2.3 Dissection and fixation of brains 18
2.2.4 Digestion and PCR genotyping 19
2.2.5 Immunohistochemistry 21
2.2.6 Bromodeoxyuridine 22
2.2.7 Histological analysis of methacrylate sections 23
2.2.8 In utero electroporation 24
2.2.9 Statistical analysis 25
3.0 Results 26
3.1 Bcl11a and Bcl11b are efficiently deleted in neocortical projection neurons of AB-mutants 26
3.2 AB-mutants show major deficits in overall neocortical architecture 28
3.3 Neocortical deep-layer neurons show disturbance in specific marker expression at P0 30
3.4 Neurogenesis in AB-mutant brains is unchanged 35
3.5 Increased cell death in embryonic stages of AB-mutant brains 36
3.6 Expression of deep-layer specific markers is severely reduced over neocortical development 37
3.7 Cell-autonomous knockout of Bcl11a and Bcl11b 42

3.7.1 In utero electroporation of Cre effectively deletes Bcl11a and Bcl11b expression in Bcl11a//b$^{flox/flox}$ neurons 43
3.7.2 In utero electroporation of Cre leads to loss of expression of deep-layer specific markers in Bcl11a//b$^{flox/flox}$ neurons 44
3.7.3 Unchanged apoptosis levels in AB-mutant neurons 46
3.7.4 Increased expression of upper-layer markers in AB-mutant neurons 47
4.0 Discussion 49
4.1 Neocortical morphology 49
4.2 Neocortical development 52
4.3 Cell-autonomous reactions 54
4.4 Prospect and future studies 56
5.0 Summary 59
6.0 Literature 60
II List of figures V
III List of tables VI
IV Acknowledgements VII
V Curriculum vitae VIII

I List of abbreviations

A-mutant	**$Bcl11a^{flox/flox}$; $Bcl11b^{flox/+;}$ $Emx1^{Cre/+}$ genotype**
AB-mutant	**$Bcl11a^{flox/flox}$; $Bcl11b^{flox/flox;}$ $Emx1^{Cre/+}$ genotype**
B-mutant	**$Bcl11a^{flox/+x}$; $Bcl11b^{flox/flox;}$ $Emx1^{Cre/+}$ genotype**
Bcl11a (transcription factor)	**B-cell lymphoma 11a**
Bcl11b (transcription factor)	**B-cell lymphoma 11b**
Brn2 (transcription factor)	**Brain 2**
CC	**Corpus callosum**
CNS	**Central nervous system**
Control	**$Bcl11a^{flox/+}$; $Bcl11b^{flox/+}$; $Emx1^{Cre/+}$ genotype**
CP	**Cortical plate**
CPN	**Cortical projection neurons**
CSMN	**Corticospinal motor neurons**
CST	**Corticospinal tract**
Cux1 (transcription factor)	**Cut like homeobox 1**
Dapi	**4',6-diamidino-2-phenylindole**
E	**Embryonic day**
Emx1 (transcription factor)	**Empty spiracles homeobox 1**
$Emx1^{Cre/+}$	**Cre-recombinase expressed under Emx1 promoter**
Fezf2 (transcription factor)	**Forebrain embryonic zinc finger-like 2**
Flox/+	**Gene is flanked by loxP sites on one allele**
Flox/flox	**Gene is flanked by loxP sites on both alleles**
Fog2 (transcription factor)	**Friend of Gata 2**
GFP	**Green fluorescent protein**
IZ	**Intermediate zone**
LP	**Lower primer**
P	**Postnatal day**
PCR	**Polymerase-chain-reaction**
Rpm	**Rounds per minute**
Satb2 (transcription factor)	**Special AT-rich binding 2**
Sox5 (transcription factor)	**Sex determining region Y box 5**
SVZ/VZ	**Subventricular zone/verntricular zone**

Tbr1 (transcription factor)	**T-box brain 1**
UP	**Upper primer**
‘	**Minutes**

1.0 Introduction

The neocortex is one of the most fascinating parts of the mammalian organism: Execution of actions, perception and integration of external and internal stimuli, the source of interactions and characteristics of our personality are located in this structure. It is the essence of us being human.

Neocortical development allows for this miraculously functioning organ, creating synaptic networks and cortical projections. But how is this important development of our neocortex being regulated? What factors define the generation of this fundamental organ that, in turn, defines us? These major questions led me to apply for an experimental doctoral thesis in neocortical anatomy and I allow myself to take pride in providing a small insight in this marvelous construct of nature.

In this thesis, I will analyse the role of the transcription factors Bcl11a (B-cell lymphoma 11a) and Bcl11b (B-cell lymphoma 11b) in neocortical development. Moreover, I will search for possible interactions between these transcription factors.

1.1 Anatomy and development of the neocortex

The histological architecture of the neocortex is organised in distinct layers formed by neurons' perykaria. The neocortex is divided in six different layers, which are counted from the neocortical surface to its ventricles.

In layer I, also called the molecular layer, inputs from different parts of the brain, e.g. the thalamus, are integrated. (Rubio-Garrido et al., 2009; Roth et al., 2016). It consists of relatively few neurons and expanded neurites.

Neocortical layers II to IV are commonly referred to as the "upper-layers" of the neocortex. The upper-layers are important for different tasks: Layer II and III form intracortical connections like the corpus callosum (Fame et al., 2011; Greig et al., 2013). Layer IV receives somatosensory inputs, e.g. in the barrel fields. These are consolidations of neurons in the neocortex where mice whiskers' afferent neurons integrate (Woolsey et al., 1970).

The neocortical layers V and VI are referred to as “deep-layers”. These deep-layers have primarily efferent tasks: Layer V contains perykaria of CSMNs (corticospinal motor neurons) (Arlotta et al., 2005; Greig et al., 2013). In layer VI, corticothalamic projection neurons are located (Hevner et al., 2001 & 2002).

All six neocortical layers are arranged parallel to the neocortical surface and vary in thickness depending on regional tasks. For example, somatomotoric segments of the brain show an increased thickness of layer V and VI, while layer IV is increased in sensory segments, like the visual cortex.

Most of the neuronal population of the neocortex can be divided in two categories: gaba-ergic, mostly inhibitory interneurons, spanning connections between neuronal networks, and glutamatergic, mostly excitatory CPNs (cortical projection neurons), whose axons lead to iso-, trans-, subcortical or subcerebral targets (Parnavelas, 2001).

Cortical projection neurons - regardless of projecting intra-, or subcerebrally - emerge from stem cell rich proliferation zones that rest on the ventricle’s surfaces. These stem cells form the SVZ/VZ (subventricular zone/ventricular zone) and begin to produce cortical projection neurons around embryonic day E10.5. Neurons born at this time form the so-called preplate. This preplate is split into two parts: The marginal zone, which forms the molecular layer (layer I) of the neocortex, and the subplate. Later born neurons are integrated between subplate and layer I, forming layers II to VI. Layers are counted outwards to inwards.

Cortical projection neurons are generated in an ‘inside-out-fashion’. Early-born neurons, i.e. born at E11.5 to E13.5 (embryonic day 11.5 to 13.5), migrate into the developing neocortex and will form the deep-layers V and VI, while neurons generated at later stages, i.e. from E 14.5 onwards., will migrate past these early-born cells to form the neocortical upper-layers II to IV (Woodworth et al., 2012; Greig et al., 2013).

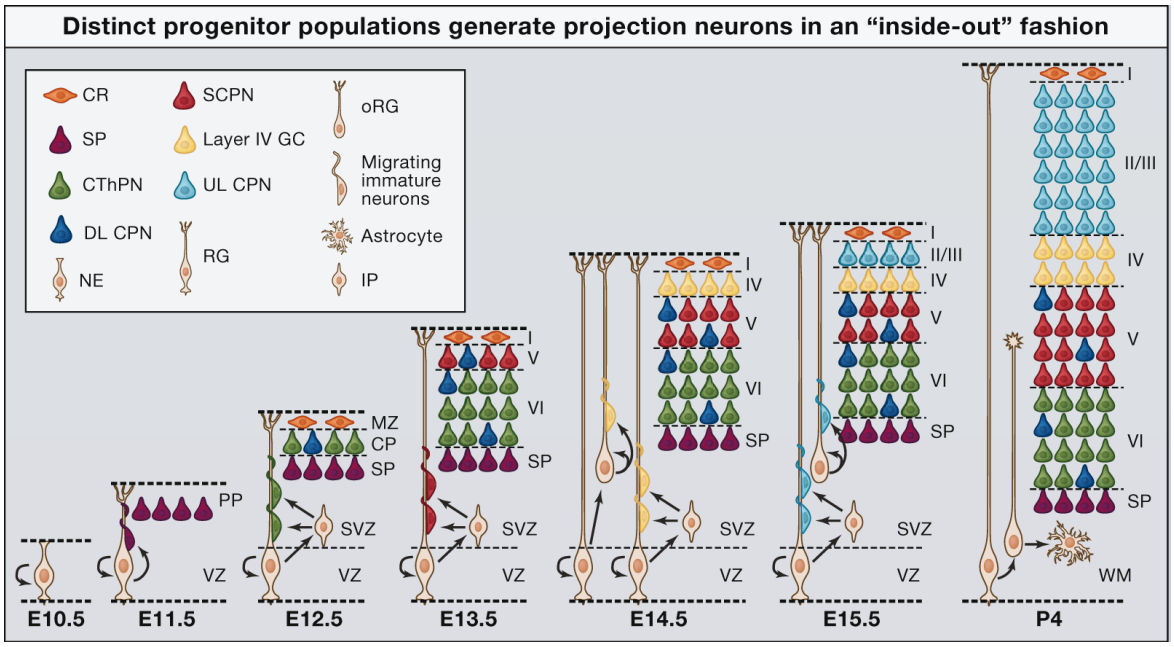


Figure 1: Distinct progenitor populations generate projection neurons in an “inside-out” fashion Neocortical projection neurons born at different embryonic stages (e.g. E10.5, E11.5) migrate into the developing neocortex: While early-born neurons inhabit deep-layers, late-born neurons migrate past and reside in upper-layers. Distinct neocortical layers are noted (latin numbers). Different types of cortical projection neurons are stated, e.g. CThPN (corticothalamic projection neurons) or DL CPN (deep-layer cortical projection neurons).

(Reprinted from: Woodworth, M. B., & Greig, L. C., Kriegstein, A. R., & Macklis, J. D. (2012). SnapShot: Cortical Development. Cell, 151, 918-918, with permission from Elsevier)

This whole process of neurons being generated, migrating, finally coming to a stop and integrating at their destination, follows a strictly defined and coordinated time schedule. The specific and elaborated sequence of events leading to a correctly formed neocortex must be maintained and hold under strict control during development of the embryo’s brain. Developing cells are led to their correct migration and specification by numerous signals. In my thesis, I will focus on members of one endogenous signal group: transcription factors.

1.2 Transcription factors

Transcription factors are proteins that share the ability to bind to DNA and increase or decrease the rate of a targeted gene's transcription. They accomplish this by binding to enhancer or silencer surrounding the gene. After binding, transcription factors form complexes with DNA. In these complexes, transcription factors interact with the downstream cascade of transcription, as well as with DNA itself.

To fulfill their role of altering gene expression, transcription factors need specialised sections to bind and interact with DNA. Via these specialised regions, or structure motifs, transcription factors can – amongst other things – be characterised and classified. Structure motifs are for example the helix-turn-helix motif, the Ets domain, or the two cysteine-two histidine zinc fingers (Latchman, 1997). Our workgroup has worked on two of these zinc finger transcription factors controlling brain development: Bcl11a and Bcl11b (John et al., 2012; Simon et al., 2012 & 2016, Wiegreffe et al., 2015).

1.2.1 Bcl11a

Bcl11a (also known as Evi9 or Ctip1) is a zinc-finger transcription factor (Avram et al. 2000) performing several different tasks in mammals. Bcl11a is not only expressed in parts of the CNS (central nervous system) such as brain and spinal cord (Leid et al., 2004; John et al., 2012), but is also essential for B- and T-lymphoid cell function (Liu et al., 2003) and its loss is associated with lymphoid malignancies (Satterwhite et al., 2001). Case reports suggest that certain genetic syndromes – e.g. the 2p15-16.1 microdeletion syndrome that is associated with microcephalus, moderate intellectual impairment and growth retardation – can possibly be caused by loss of Bcl11a (Hancarova et al. 2013).

Regarding the neocortex, Bcl11a is expressed throughout the neocortical layers I to VI (Wiegreffe et al., 2015). It has been shown that Bcl11a is of great importance for correct migration and specification of neurons. Loss of Bcl11a leads to a shrinkage in cortical thickness and influences upper-layer formation (Wiegreffe et al., 2015). The authors discuss that this disturbance in formation leads to observed massive apoptosis.

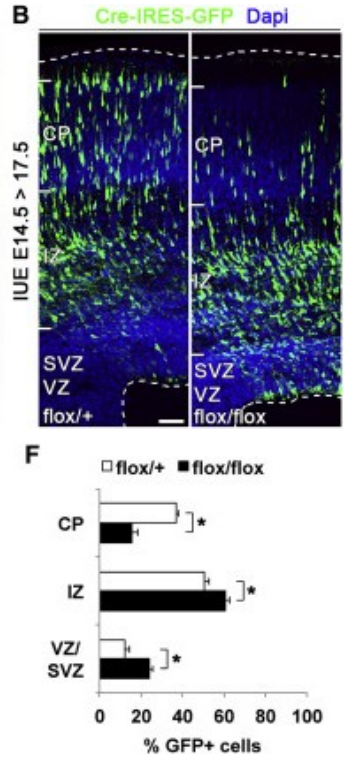


Figure 2: Bcl11a deficient neurons fail to migrate correctly

The right column (annotated flox/flox) shows neurons (green, annotated Cre-IRES-GFP) lacking Bcl11a (B-cell lymphoma 11a) have severe defects in neuronal migration compared to control neurons (left column, annotated flox/+). Neurons were analysed on day 17 of embryogenesis (E17.5) and transfected with the mutation on E14.5. The graph depicts the percentages of cells distributed CP (cortical plate), IZ (intermediate zone) and VZ/SVZ (subventricular zone /ventricular zone). Higher percentage of neurons in deeper structures (i.e. IZ, VZ/SVZ) indicates neurons' disability of migrating correctly. The graph depicts means, standard errors of the mean are shown by whiskers, *$p < 0.05$.

(Reprinted from: Wiegreffe, C., Simon, R., Peschkes, K., Kling, C., Strehle, M., Cheng, J., Srivatsa, S., Liu, P., Jenkins, N. A., Copeland, N. G., Tarabykin, V., & Britsch, S. (2015). Bcl11a (Ctip1) Controls Migration of Cortical Projection Neurons through Regulation of Sema3c. Neuron, 87, 311-325, with permission from Elsevier)

In neocortical deep-layers, Bcl11a orchestrates correct composition of subcerebral projection neurons (Woodworth et al., 2016), amongst others via repression of another transcription factor, Tbr1 (T-box brain 1) (Cánovas et al., 2015). Bcl11a specifies areas of the neocortex: it represses motor cortex formation and enhances construction of sensory neocortical areas (Greig et al., 2016; Woodworth et al., 2016). Upon deletion, layer VI corticothalamic projection neurons show disturbed projections. Further it has been shown that axon and dendrite outgrowth is regulated via interaction of different Bcl11a isoforms (Kuo et al., 2009).

1.2.2 Bcl11b

Bcl11b (also known as Ctip2) is a zinc-finger transcription factor (Avram et al., 2000) that – like the closely related Bcl11a – executes different functions in mammalian organisms. It is found in parts of the CNS such as the neocortex, cerebellum, striatum (Leid et al. 2004) and hippocampus (Simon et al., 2012), whilst it also plays a critical role in the formation of T-lymphocytes (Tydell et al., 2007) and other lymphoid cells (Califano et al., 2015).

Bcl11b is expressed in neocortical layers V and VI (Molyneaux et al., 2007) and is required for different events during neocortical development. It has been shown that the development of the CST (corticospinal tract) is dependent on Bcl11b (Arlotta et al., 2005). Bcl11b mutants are unable to form a functional connection of brain to CST, as it stops at pons level.

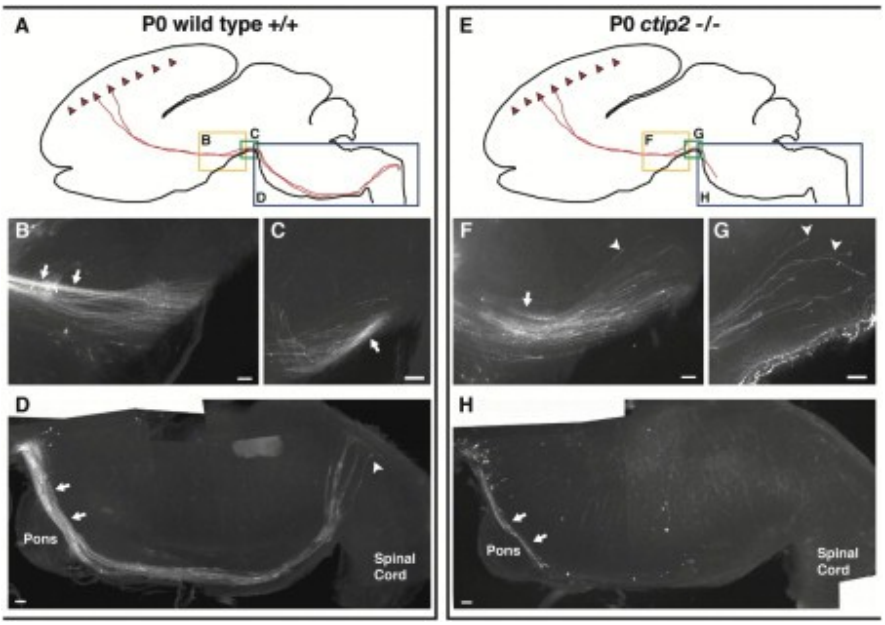


Figure 3: **Bcl11b mutants do not manifest a corticospinal tract (CST) (Arlotta et al., 2005)**
Mutants lacking Ctip2 (=Bcl11b) (B-cell lymphoma 11b) (E, magnifications in F-H), are compared to wild-types (A, magnifications in B-D) on their first day of life (P0). In mutants, the CST (corticospinal tract) stops at the level of the pons, and does not connect to the spinal cord (H). Arrows show neuronal projections, anatomical landmarks are noted.

(Reprinted from: Arlotta, P., Molyneaux, B. J., Chen, J., Inoue, J., Kominami, R., & Macklis, J. D. (2005). Neuronal subtype-specific genes that control corticospinal motor neuron development in vivo. Neuron, 45, 207-221, with permission from Elsevier)

Furthermore, Bcl11b mutants die soon after birth (Arlotta et al., 2005) if the knockout is not restricted to specific areas of the brain.

Bcl11b is essential for correct specification of different cortical projection neuron (CPN) classes, performing this via repressing or enhancing other transcription factors like Satb2 (Special AT-rich binding 2), Fezf2 (Forebrain embryonic zinc finger-Like 2) or Tbr1. (McKenna et al., 2011; Srinivasan et al., 2012). If altered, correct axonal projection (subcortical, subcerebral or transcortical) of deep-layer neurons is disturbed.

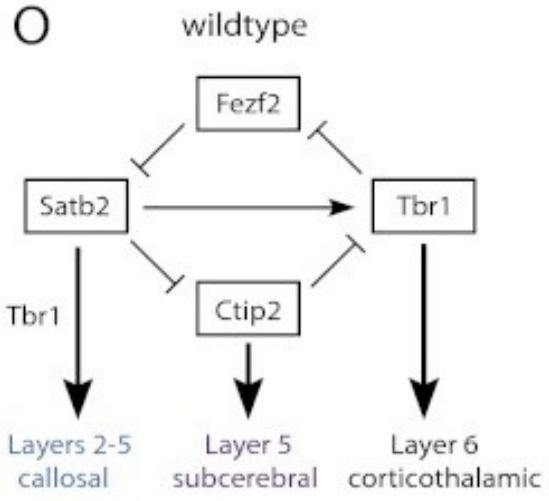


Figure 4: **Model of transcription factors directing neuronal projection differentiation (Srinivasan et al., 2012)**

Neuronal projections are regulated by Ctip2 (=Bcl11b) (B-cell lymphoma 11b), Tbr1 (T-box brain 1), Satb2 (Special AT-rich binding 2) and Fezf2 (Forebrain embryonic zinc finger-like 2). The different transcription factors repress and directly enhance each other, leading to different axonal targeting.

(Reprinted from: Srinivasan, K., Leone, D. P., Bateson, R. K., Dobreva, G., Kohwi, Y., Kohwi-Shigematsu, T., Grosschedl, R., & McConnell, S. K. (2012). A network of genetic repression and derepression specifies projection fates in the developing neocortex. Proceedings of the National Academy of Sciences, 109, 19071-19078, with permission from PNAS)

1.2.3 Deep-layer specific transcription factors

To analyse the influence of Bcl11a and Bcl11b on neocortical deep-layers, I investigate the expression of deep-layer specific transcription factors:

Fog2 (Friend of Gata 2) is a transcription factor that is primarily expressed in the neocortical layer VI. It plays an important role in the function of corticothalamic projection neurons, guiding and maintaining their correct specification and targeting (Galazo et al., 2016).

The transcription factor Sox5 (Sex determining region Y box 5) is primarily expressed in the neocortical layers V and VI. It is important for correct specification of projection neurons. If lost, corticothalamic projection neurons' differentiation is impaired and connectivity of subcerebral projection neurons is disturbed (Lai et al., 2008; Kwan et al., 2008).

Tbr1 is a transcription factor that is temporarily expressed in all projection neurons during embryonic development, but resides to a strong expression in layer VI at about P0 (postnatal day zero). Loss of Tbr1 results in mis-differentiation of CPNs, their projections form Probst bundles, and cortical layer formation is disturbed (Hevner et al., 2001 & 2002; McKenna et al., 2011).

1.2.4 Upper-layer specific transcription factors

I analysed neuronal mis-specification using upper-layer specific transcription factors:

Brn2 (Brain 2) is a transcription factor specifically expressed in neocortical upper-layers. It is important for forming the corpus callosum (Oishi et al., 2016).

Cux1 (Cut like homebox 1) is primarily expressed in neocortical layers II to IV and is important for forming the corpus callosum (Rodríguez-Tornos et al., 2016).

Satb2 (Special AT-rich binding 2) is a transcription factor that is expressed in both upper-layer and deep-layer neurons. It executes tasks like formation of the corpus callosum in upper-layers, and is important for correct specification of subcerebral projections in deep-layers (Srinivasan et al., 2011; Leone et al., 2015).

1.3 Aims of my thesis

Bcl11a and Bcl11b are both essential genes for the correct development of the neocortex. Multiple studies show their importance for neocortical development by knockout/knockdown experiments. (Arlotta et al., 2005; McKenna et al., 2011; Srinivasan et al., 2012; Wiegreffe et al., 2015; Cánovas et al., 2015).

Bcl11a and Bcl11b are related, highly conserved genes of the Bcl11 C_2H_2 zinc finger protein family (Avram et al., 2000). Bcl11a even belongs to the group of 'ultraconserved elements', i.e. it has a 100% identity with mouse or rat genome for at least 200bp (Bejerano et al., 2004). Bcl11a can be traced back to Drosophila melanogaster, showing 100% identity in coding exons (Bejerano et al., 2004). As Bcl11a did not undergo major evolutionary changes during development of different species, on can assume it has a critical function in organisms.

Satterwhite et al. (2001) showed that Bcl11a and Bcl11b feature a homology of amino acids up to 61%. Moreover, they share 95% identity of proline-rich and acidic regions in their operational DNA-binding structure motifs, their C_2H_2 zinc fingers (Satterwhite et al., 2001).

According to literature, Bcl11a and Bcl11b are expressed at different parts of the brain (Leid et al., 2004). Interestingly, expression of Bcl11a and Bcl11b overlaps in neocortical layers. As mentioned, Bcl11a is expressed throughout neocortical layers II to VI (Wiegreffe et al., 2015) while Bcl11b is mostly restricted to layers V and VI (Molyneaux et al., 2007). Woodworth et al. (2016) showed that deep-layer neurons co-express Bcl11a and Bcl11b to various extents. Further it has been shown that both genes influence neuronal projections in neocortical deep-layers (Cánovas et al., 2015; McKenna et al., 2011; Srinivasan et al., 2012; Woodworth at el., 2016).

In this thesis, I analyse the role of Bcl11a and Bcl11b on neocortical development. To examine their influence on the evolving neocortex, I use Bcl11a; Bcl11b double-knockout mice. Literature research indicates neocortical deep-layers as a site of considerable double-knockout phenotype, as both transcription factors operate in this area (Woodworth et al., 2016; Cánovas et al., 2015; Wiegreffe et al., 2015; Molyneaux et al., 2007; Arlotta et al., 2005).

Furthermore, I investigate possible interactions of the transcription factors Bcl11a and Bcl11b: Bcl11a and Bcl11b are closely related, Bcl11a has not undergone major changes in evolution, both transcription factors are expressed in neocortical deep-layers and both perform tasks in differentiation of deep-layer neurons. This context raises the question whether there are possible interactions between these transcription factors. Can these highly conserved genes that are expressed in overlapping areas at least partially execute functions of its counterpart, thus compensate for the loss of each other?

To address for these questions, I knock out Bcl11a and Bcl11b simultaneously, and compare these double-mutants to mice lacking either Bcl11a or Bcl11b. If the phenotype of the double-knockout mice is influenced more strongly than the phenotypes of Bcl11a-mutants and Bcl11b-mutants taken together, this indicates compensatory abilities of Bcl11a and Bcl11b.

2.0 Materials and Methods

2.1 Materials

Table 1: Chemicals

Chemicals	*Company*	*Catalog no.*
Acetic acid ($C_2H_4O_2$)	Sigma Aldrich	UN2798
Agarose	Lonza	50004
Bromodeoxyuridine (BrdU) ($C_9H_{11}BrN_2O_5$)	Sigma Aldrich	B9285
Bromophenol	Sigma Aldrich	114405
Cresyl violet acetate	Waldeck	1A-400
D(+)Sucrose ($C_6H_{12}O_6$)	AppliChem Panreac	A2211,1000
Di-sodium hydrogen phosphate heptahydrate ($Na_2HPO_4*7H_2O$)	Merck	1.06575.1000
Diethyldicarbonate (DEPC) ($C_6H_{10}O_5$)	Roth	K.028.2
dNTPs	Invitrogen	55082-55085
Dapi ($C_{16}H_{15}N_5$)	Thermo Fischer	D1306
EDTA	Merck	1.08455.0250
Entellan	Merck	1.07961.0500
Ethanol (C_2H_6O)	Sigma Aldrich	32205
Ethidiumbromide ($C_{21}H_{20}BrN_3$)	Roth	7870.2
Glycerol	Sigma Aldrich	15523
Horse-Serum (HS)	Sigma Aldrich	H0146
Hydrogen Chloride (HCl)	Sigma Aldrich	30721
Hyper Ladder IV	Bioline	BIO-33056
Magnesium chloride ($MgCl_2$)	Invitrogen	564749
Nitrogen (N_2)	Linde	4130919
Paraformaldehyd (PFA) $OH(CH_2O)_nH$ (n=8-100)	AppliChem Panreac	A3813,1000
PCR-buffer (10x)	Invitrogen	1315052
Potassium chloride (KCl)	Merck	1.04936.1000
Proteinase K	Roche	12949200

Sodium azide (NaN_3)	AppliChem Panreac	A1430,0500
Sodium chloride (NaCl)	Sigma Aldrich	SZBE0630V
Sodiumdihydrogen phosphate monohydrate ($NaH_2PO_4*H_2O$)	Merck	1.06346.1000
Sodium dodecyl sulfate (SDS) ($NaC1_2H_{25}SO_4$)	Roth	4360.2
Sodium hydroxide (NaOH)	Merck	1.06495.1000
Taq-Polymerase	Invitrogen	100021276
Technovit-7100 kit	Kulzer	64709003
Tri-Sodium citrate dihydrate ($C_6H_5Na_3O_7*H_2O$)	AppliChem	A2403,1000
Tris	Sigma	BCBL9102V
Triton	AppliChem Panreac	A4975,0500
Xylen cyanol	Roth	A513.1
Xylene substitute	Sigma Aldrich	A5597

Table 2: Solutions

Solution	*Ingredients*
BrdU	10 mg/ml BrdU 0.9% NaCl
DEPC-PB (0.2M)	0.155M $Na_2HPO_4*_7H_2O$ 0.046M $NaH_2PO_4*H_2O$ 0.01% $C_6H_{10}O_5$ pH 7.2
DEPC-H_2O	Milli-Q H_20 0.01% $C_6H_{10}O_5$
DEPC-PBS	PBS 0.01% $C_6H_{10}O_5$
Loading buffer	30% Glycerol 0.2% Xylen cyanol 0.2% Bromophenol

PBS	0.014M NaCl 0.003M KCl 0.005M Na_2HPO_4 0.0003M KH_2PO_4 pH 7.4
PBTx	0.1% Triton DEPC-PBS
PFA (4%)	4% Paraformaldehyde 0.1M DEPC-PB
Sodium citrate-buffer	10mM $C_6H_5Na_3O_7*2H_2O$ pH 6.0
Sucrose/PB	20% sucrose 0.1M DEPC-PB
TAE-buffer	0.4M Tris 0.01M EDTA 11.42 ml $C_2H_4O_2$ pH 8.0
Tail-buffer	100mM Tris pH 8.5 5mM EDTA pH 8.0 0.2% SDS pH 7.2 200mM NaCl

Table 3: Primers

Primer	*Sequence*	*Company*
Bcl11aflox upper primer (UP)	TAGCTCCTGCTAGCCAGGTTTCTT (5'-3')	Eurofins genomics
Bcl11aflox lower primer (LP)	CGAGGCTTGCAGAAACAGAAAGAT (5'-3')	Eurofins genomics
Bcl11bflox UP	TGAGTCAATAAACCTGGGCGAC (5'-3')	Eurofins genomics
Bcl11bflox LP	GGAATCCTTGGAGTCACTTGTGC (5'-3')	Eurofins genomics
Emx1Cre UP	GTATTTGGTTTAGAGTTTGGC (5'-3')	Eurofins genomics
Emx1Cre LP	GGGGGACATGCGAGGATGTCA (5'-3')	Eurofins genomics

Table 4: Antibodies

Antigen	*Host*	*Dilution*	*Company / catalog no.*
Bcl11a	rabbit, polyclonal	1:1250	Institute of Molecular and Cellular anatomy, University of Ulm
Bcl11b	guinea-pig, polyclonal	1:1250	Institute of Molecular and Cellular anatomy, University of Ulm
BrdU	rat, monoclonal	1:700	AbD Serotec, OBT0030
Brn2	goat, polyclonal	1:100	Santa-Cruz, sc-6029
Cleaved caspase 3	rabbit, polyclonal	1:250	Cell Signaling, ASP175
Cux1	rabbit, polyclonal	1:500	Santa Cruz, sc-13024
Fog2	rabbit, polyclonal	1:250	Santa Cruz, sc-10755
Sox5	rabbit, polyclonal	1:300	GenWay Biotech, GWB-73C04A
Tbr1	rabbit, polyclonal	1:500	Abcam, ab31490

Table 5: Devices

Device	*Company*	*Model*
Confocal microscope	Leica	TCS SP5 II
Cryostat	Microm	HM560
Fluorescent microscope	Leica	Leica CTR 6000
Gel-Electrophoresis chamber	Peqlab	EV261
Microtome	Thermo	MicromHM355S
PCR-cycler	Biometra	Thermocycler 3000
Stereo microscope	Leica	5880974
UV-chamber	Peqlab	BioVis 3026
Water purifier	Millipore	Milli-Q Plus water system

2.2 Methods

2.2.1 Cre/loxP system

In my thesis, I analyse the phenotype of Bcl11a and Bcl11b double-mutant mice. As a germline mutation of Bcl11a or Bcl11b is perinatally lethal (Liu et al., 2003; Wakabayashi et al., 2003; Arlotta et al., 2005) a method inducing the knockout specifically in the forebrain region is needed. The target knockout is accomplished by using the Cre/loxP system, first described by Dr. Brian Sauer in 1987 (Sauer, 1987), and first described in mice specifically 1994 by a different workgroup (Gu et al., 1994). By using a specific promoter that controls the expression of Cre-recombinase it is possible to knock out genes in certain regions - e.g. the forebrain or hippocampus - while leaving expression in the remaining organism intact.

I used the Cre/loxP system to knock out Bcl11a and Bcl11b specifically in the forebrain. The Cre-recombinase is under control of the Emx1 (empty spiracles homeobox 1) promoter, which is active in progenitors of glutamatergic projection neurons of the telencephalon (Gorski et al., 2002).

In the Cre/loxP system, distinctly marked sequences of DNA are cut out by the Cre-recombinase. DNA-sequences are marked by adding so called loxP sites up- and downstream. If present, Cre-recombinase is able to detect these sequences in the DNA-strand. It excises one loxP site and the DNA-sequence flanked by the loxP sequences. It is important to know that the addition of loxP sites alone does not alter the expression of a target gene significantly. A knockout only results if combined with Cre-recombinase (Li et al., 2010).

Whether a targeted gene is flanked by loxP sites (annotated ^{flox}) on one or both alleles decides for the animal's genotype: Flox/flox; Cre/+ animals have the targeted gene cut out in both alleles, so no gene expression is present. Flox/+; Cre/+ animals keep one intact copy of the targeted gene.

2.2.2 Gene-modified animals and mating system

Bcl11a^{flox} mice were generated by P. Liu (Liu et al., 2003) and have previously been used by our working group (John et al., 2012; Wiegreffe et al., 2015). LoxP sites flank the first exon of Bcl11a, which results in a loss of expression of Bcl11a if Cre-recombinase is present.

Bcl11b^{flox} mice were generated by P. Li (Li et al., 2010) and have also been used by our working group (Simon et al., 2012 & 2016). Exons 4-6 are flanked with loxP-sites, resulting in a deletion of Bcl11b.

Emx1-Cre mice were generated by J. A. Gorski (Gorski et al., 2002). Under control of this promoter, Cre-recombinase is activated in progenitors of cortical projection neurons of the telencephalon.

To analyse mice with a Bcl11a and Bcl11b double-mutant phenotype, I mated Bcl11a$^{flox/flox}$; Bcl11b$^{flox/flox}$ females (also annotated Bcl11a//b$^{flox/flox)}$ with Bcl11a$^{flox/+}$; Bcl11b$^{flox/+}$; Emx1$^{Cre/+}$ males. These females and males do not show any abnormalities. The double-mutants have a Bcl11a$^{flox/flox}$; Bcl11b$^{flox/flox}$; Emx1$^{Cre/+}$ genotype. They will be referred to as AB-mutants in my thesis.

The control animal has a Bcl11a$^{flox/+}$; Bcl11b$^{flox/+}$; Emx1$^{Cre/+}$ genotype. As mentioned before, loxP-sites alone do not result in a change of gene expression (Li et al., 2010). Accordingly, all littermates lacking Emx1Cre are regarded as controls, with no further analysis of their loxP-site distribution (e.g. Bcl11a$^{flox/flox}$; Bcl11b$^{flox/+}$; Emx1$^{+/+}$). These genotypes will be referred to as Controls.

Mice lacking either Bcl11a or Bcl11b are also used in this study. Bcl11a$^{flox/flox}$; Bcl11b$^{flox/+}$; Emx1$^{Cre/+}$ will be referred to as A-mutants, while Bcl11a$^{flox/+}$; Bcl11b$^{flox/flox}$; Emx1$^{Cre/+}$ mice will be referred to as B-mutants.

All experiments involving mice were carried out in accordance with the German law and have been approved by respective government in Tuebingen, TV 1197, o.161.

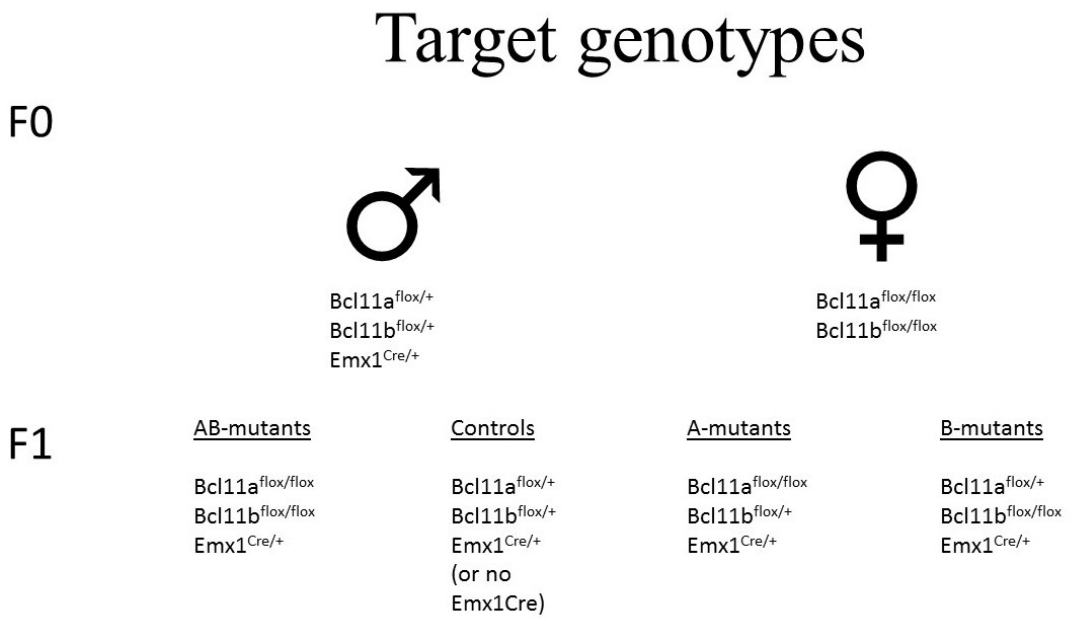


Figure 5: **Genotypes used in this thesis**

F0 shows genotypes of parental mice, F1 the genotypes of their offspring. Note that controls either have a $Bcl11a^{flox/+}$; $Bcl11b^{flox/+}$; $Emx1^{Cre/+}$ genotype or any distribution of loxP-sites, as long as no Emx1Cre is present.

2.2.3 Dissection and fixation of brains

After sacrificing the mother, littermates were put in ice-cold PBS at the same time to guarantee equal timepoints of analysis.

Dissection of animals began with decapitation. Afterwards, while holding the head at the orbitae, the skin of the skull was incised along the median line and peeled off. The skull itself was opened along the sagittal suture, and two orthogonal cuts were made at the level of the ears, allowing removal of the calvarium without damaging the brain. The brainstem and the bulbi olfactorii were cut, hence the brain could be carefully extracted out of the skull. Brains were put in ice-cold 4% PFA/PBS and stored at 4°C. The fixation with PFA lasted one night. For genotyping of the dissected animals, a small piece of tail or yolk sack was used.

Dissected brains stored overnight in 4% PFA/PBS were washed three times with PBS for 10'. This washing assures that all PFA is displaced and thus fixation is ended. Brains were stored in PBS containing 0.01% NaN_3 at 4°C. NaN_3 prevents decay of the brains. For long-time storage, brains were put in a 20% sucrose/PBS solution overnight, and were frozen

afterwards in plastic wells in tissue freezing medium. It proved efficient to freeze and store AB-mutants together with controls and A-mutants together with B-mutants in the same wells. This allowed for same staining conditions in the following processes. Frozen brains were kept at -80°C.

2.2.4 Digestion and PCR genotyping

For DNA-retrieval, tails were digested in tail buffer containing 1% Proteinase K and put in a 55°C shaking incubator for 2 hours. The Proteinase K digests the cells so the DNA leaks into the solution. Afterwards, Proteinase K is inactivated by putting the sample to 95°C for 10'. This step is critical because the Proteinase K would also digest the Taq-polymerase added for subsequent PCR (Polymerase-chain-reaction) genotyping. After inactivation, the digestion solution was diluted in 200µl Milli-pore H_2O. To allow for clean handling and to minimize the risk of cross-contamination, the samples were spun down in a centrifuge for 60 seconds at 15000rpm.

Genotyping was performed via PCR, first described by R. K. Saiki in 1985 (Saiki et al., 1985). The characteristic of the Taq-polymerase surviving high temperatures allows heating the samples to 97°C, where dissociation of both DNA-strands occurs. The sample is cooled down to 55°C, allowing primers designed specifically to fit to the target gene areas to bind. Reheated to 72°C, Taq-polymerase adds dNTPs to the end of the primers, thus synthesizing a copy of the target gene. These steps are repeated multiple times, resulting in an exponential increase of target gene copies.

A 'mastermix' with all reagents except DNA-templates was prepared and put into PCR-tubes. Afterwards, DNA-samples were added, the tubes closed and mixed, spun down shortly and put into the PCR-cycler. To check for genotyping mistakes or contamination, defined positive and negative control samples were added to each PCR.

Table 6: Ingredients of different PCRs

Reagents / [µl]	***Emx1Cre***	***Bcl11a$^{flox/+}$, Bcl11b$^{flox/+}$***
H_2O	21,4	13,2
PCR-buffer	3	2
dNTPs	1,5	1
Upper primer	1	1
Lower primer	1	1
$MgCl_2$	0,9	0,6
Taq-polymerase	0,2	0,2
DNA-template	1	1
Total	30	20

Evaluation of specimen's genotype was done using gel-electrophoresis. Agarose was diluted in TAE-buffer to a 1% solution and warmed in a microwave oven until completely dissolved. 2-3 drops of ethidiumbromide were added to each 100ml gel allowing better analysis later on.

After the gel was completely loaded with all samples - each of them mixed with a drop of loading buffer - a "hyper ladder" was added separately. This hyper ladder is a mixture of base-constructs with a defined length to allow the analysis of amplicon length later.

For 35', an electric field of 230V and 35W was applied to the gel. In this process, the ethidiumbromide mixes with the amplified bands and can be seen under UV-exposure. The longer the length of the amplified band, the slower its migration speed in the gel. Samples can be examined for their genotype comparing migration distance – which correlates with amplified band length – to the defined hyper ladder.

2.2.5 Immunohistochemistry

IHC (immunohistochemistry) is a technique in which target proteins are marked and labeled via antibodies. In my thesis, I always used two types of antibodies: The primary antibody binds to the targeted protein on the brain section itself, while the second antibody, which is conjugated with a fluorophore, binds to the primary one. Analysis can be done via measuring fluorophore-specific light emission at a certain wavelength.

Sections were cut in a thickness under 20µm. This was achieved by using a cryostat. The cryostat can cut extremely thin sections at negative temperatures, and sections melt to a glass slide stored at room temperature. Sections were prepared at -18°C to -20°C and had a thickness of 12µm to 14µm. From each brain, parallel series of sections were produced, ranging from 4 to 6 series, which allowed multiple stainings in similar regions of the same brain.

After cutting the brain, glass slides with attached sections were dried at room temperature for 1 hour and stored at -80°C until IHC.

The staining procedure started with thawing the frozen slides for 30' and encircling the sections with a fatty pen. This encircling ensured that later added solutions reside on the sections. After the slides were washed in PBS two times for 10', sodium citrate buffer was added and they were put in a steam chamber filled with Milli-pore H_2O for 2'. Steaming the sections in sodium citrate buffer allowed for better results in staining as it clears occlusions of target antigens that may arose during brain fixation. Slides were left at room temperature to cool down for 5' and were put in PBTx two times for 10'.

Sections were blocked with 10% HS (horse serum) in PBTx for 1 hour at room temperature. The blocking solution was added to minimize binding of antibodies to unspecific epitopes. After blocking, the primary antibody solution diluted in 5% HS in PBTx was added and left to incubate at 4°C overnight. Primary antibodies bind to the target protein itself.

The following day, antibodies were washed away using 5% HS in PBTx three times for 10'. After the third washing step, the secondary antibodies and Dapi (4',6-diamidino-2-phenylindole) were added, again diluted in 5% HS in PBTx. The secondary antibody is conjugated with a fluorophore and binds to the primary antibody already connected to the target protein. Dapi binds to A-T rich sequences of DNA in tissue sections (Kapuscinski, 1995). In all experiments in of this thesis, Dapi was added in a 1:5000 solution. The solution containing secondary antibody and Dapi stayed on the sections for 120' at room temperature. Afterwards, slides were washed three times for 5' in PBS, briefly dipped in water to flush remaining reagents out, and mounted using immunomount and a cover slip. After drying for 1 hour, slides were sealed with nail varnish and stored until analysis at 4°C. The air-tight sealing with nail varnish allowed longer storing of the slides.

2.2.6 Bromodeoxyuridine

The thymidine-analogon BrdU (Bromodeoxyuridine) is a substrate that is integrated in DNA of cells undergoing cell-division. With distinct antibodies against BrdU it is possible to mark cells undergoing cell-division or being successors of dividing cells (Cooper-Kuhn et al., 2002). A cell incorporating BrdU during division will pass parts of it to its daughter cell, who in turn distributes it again after cell cycle. By adding BrdU to a pregnant mouse and leaving it for an exactly defined length of time (called "pulse-chase"), it is possible to compare neurogenesis rates of mutants and controls in the same experiment. Mice were sacrificed 30' after BrdU injection and to stop further cell division embryos were put in ice-cold PBS immediately. In each experiment, the same concentration of 50mg per kg of the mother's body weight was used.

For the analysis of neurogenesis, pregnant mice were injected with BrdU exactly 30' before they were sacrificed.

The prewarmed BrdU-solution was carefully injected into the mother's abdominal cavity. BrdU-stainings were performed in a similar manner to other IHC-stainings:

After thawing, slides were postfixed in 4% PFA/PBS for 10' at room temperature, washed in PBS for 5' three times, and incubated in pre-warmed 2M HCl solution for 15' at 37°C. Afterwards, possible HCl remnants were washed away in PBS, and slides were put into PBTx two times for 10'. Blocking was performed with 10%HS in PBTx for 1 hour at room temperature.

The BrdU antibody was applied and left to incubate overnight at 4°C. The next day, a secondary antibody and Dapi were added. Sections were further treated as described in the IHC-protocol.

2.2.7 Histological analysis of methacrylate sections

For preparation of methacrylate sections, brains were fixed in 4% PFA/PBS at 4°C for 72 hours. Brains were washed several times with PBS for 48 hours, and afterwards dehydrated in an ascending ethanol series (25%, 50%, 75%, 95% and 100%) diluted in PBS at 4°C for 2 days at each step. Pre-infiltration was done by mixing 100% ethanol with Technovit base solution 7100 (1:1 ratio) and incubating brains in this solution for 48 hours at room temperature. For infiltration, brains were put in Technovit base solution for 48 hours at room temperature. Brains were embedded in an upright position as they were put into a plastic mold. This plastic mold was afterwards filled with Technovit polymerization solution, and left under a fume hood to dry for 24 hours. The methacrylate block was stored at room temperature.

Methacrylate-embedded brains were cut with a microtome at 5 µm thickness. After cutting, sections were carefully stretched onto glass slides in a water bath. 4 to 6 sections were left to dry on each slide. For my analysis, I used every 4^{th} to 6^{th} section.

All methacrylate sections in this study were stained with cresyl violet (Nissl-staining). For test stainings sections from posterior brain levels were used.

The sections were left in the staining solution for 2 minutes. Staining solution consisted of 0.1% cresyl violet and Walpole buffer (1:5 dilution). After staining, sections were washed 6 times for 150 seconds in distilled water, and were left to dry at 37°C for 30 minutes. Optimal contrast was achieved by carefully rinsing the slides multiple times in 70% ethanol.

After checking the staining quality and contrast under a microscope, slides were put under a fume hood to dry at room temperature overnight. Slides were mounted with a coverslip and sealed with entellane. Slides were stored at room temperature.

2.2.8 *In utero* electroporation

With using IUE (*in utero* electroporation), it is possible to create a genetic mosaic situation, i.e. generate isolated genetically modified cells in a wild-type genetic background (Saito et al., 2001).

Neuronal progenitor cells are transfected with a DNA vector (for example containing Cre). This vector also expresses a fluorescent reporter protein, such as GFP (green fluorescent protein), which allows distinguishing transfected versus not transfected cells. In this study, IUE experiments were executed at E12.5 on Bcl11a//b$^{flox/flox}$ animals. The mother was anaesthetised with isoflurane. The abdominal cavity was opened, and the uterine horns were taken out. 2 µL of DNA vector were injected into each embryonic brain. Via electrodes, a voltage field was applied to the brain. 5 pulses of 35 volts and 50 ms duration were applied. After all embryos had been electroporated, the uterine horns were put back into the mother's abdominal cavity and closed by suture.

Transfected brains were analysed at P0. In one experiment, the vector only expressed GFP, so just "control brains" were generated (later on annotated IRES-GFP), while in a similar experiment, brains were transfected with a vector expressing GFP and the Cre-recombinase, thus leading to "mutant brains" (later on annotated Cre-IRES-GFP). Brains were analysed with IHC already described.

2.2.9 Statistical analysis

All images that were used for statistical quantification were taken on a confocal microscope (TCS SP5 II, Leica). The confocal microscope irradiates sections with light of defined wavelengths. Secondary antibodies are connected to a fluorophore, which is excited at a distinct wavelength. This allows for analyses of several proteins marked with different fluorophores on the same section.

Brain sections were matched using Atlases of Anatomy by Kaufman, M. H. (1992) and Paxinos, G., & Keith, F. (2012).

Cell counting was done using Photoshop 4 (Adobe). In each experiment, cells were counted in a radial unit, that was orientated orthogonal to the brains surface and ventricles. P0 radial units measured 350µm, BrdU expression was analysed in radial units of 150µm. Marker expression on E11.5, E12.5 and E13.5 was examined in units of 200µm, while this units extended to 350µm on E15.5 and E17.5. Cleaved caspase 3 signal was counted in radial units of 300µm from E11.5 on to E13.5, and in units of 700µm from E15.5 on to P0. IUE experiments were evaluated in radial units of 200µm, and 300µm for apoptosis signal, respectively.

Images for analysis were corrected for brightness and contrast. Controls and mutants were counted using the same brightness, contrast and threshold settings. BrdU stainings were not contrasted before the analysis, to minimize chances of miscounting cells.

From each brain, at least three sections were analysed. Each experiment that was quantified contained at minimum three control and three mutant brains. Experiments for qualitative purposes were only performed on two control and two mutant brains, again with at least three sections of each brain analysed.

Quantification and statistical analysis were carried out with Excel (Microsoft) and SPSS (IBM) software.

All statistical analyses were executed using student's t-test, normal distribution was assumed. Significant results are annotated with *($p<0.05$), **($p<0.01$) and ***($p<0.001$), n.s. marks non-significant results. Standard errors of the mean are stated. From each brain at least three anatomically matched sections were analysed and a mean for the brain was calculated. Results were quantified using these means.

3.0 Results

3.1 Bcl11a and Bcl11b are efficiently deleted in neocortical projection neurons of AB-mutants

In this study, I describe the phenotype of Bcl11a and Bcl11b double-mutant mice. The first experiment I did was to check whether the knockout of Bcl11a and Bcl11b works efficiently in cortical projection neurons.

In figure 6, typical expression levels of both transcription factors are shown in control, A-, B-, and AB-mutant P0 frontal sections. A-mutants still express Bcl11b, and B-mutants still express Bcl11a, respectively.

In control brains, Bcl11a shows an expression throughout the neocortical layers II-VI, while Bcl11b is restricted to the deep neocortical layers V and VI. These expression profiles coincide with literature (Wiegreffe et al., 2015; Molyneaux et al., 2007). In the neocortical deep-layers, many cells co-express Bcl11a and Bcl11b (see yellow cells in figure 6, most notably in box I') to various extents.

In A-mutants, Bcl11a expression is hardly detectable, except in a few cells that are most likely interneurons not influenced in gene expression by the Emx1 promoter. Overall thickness of the neocortex is slightly decreased, as well as the number of Bcl11b positive cells appears to be increased, according to literature (Wiegreffe et al., 2015).

In B-mutants, Bcl11a expression seems not to be altered compared to controls, while Bcl11b protein expression is almost not detectable. Cortical thickness of B-mutants appears to be at the same level as in control brains.

In AB-mutants, expression of both transcription factors is hardly detectable. Only a few scattered cells express Bcl11a. As mentioned above, these cells are most likely interneurons. Loss of expression of either transcription factor shows that the genetic knockout strategy is highly efficient. Note the enormous shrinkage of overall cortical thickness, suggesting major changes in neocortical architecture.

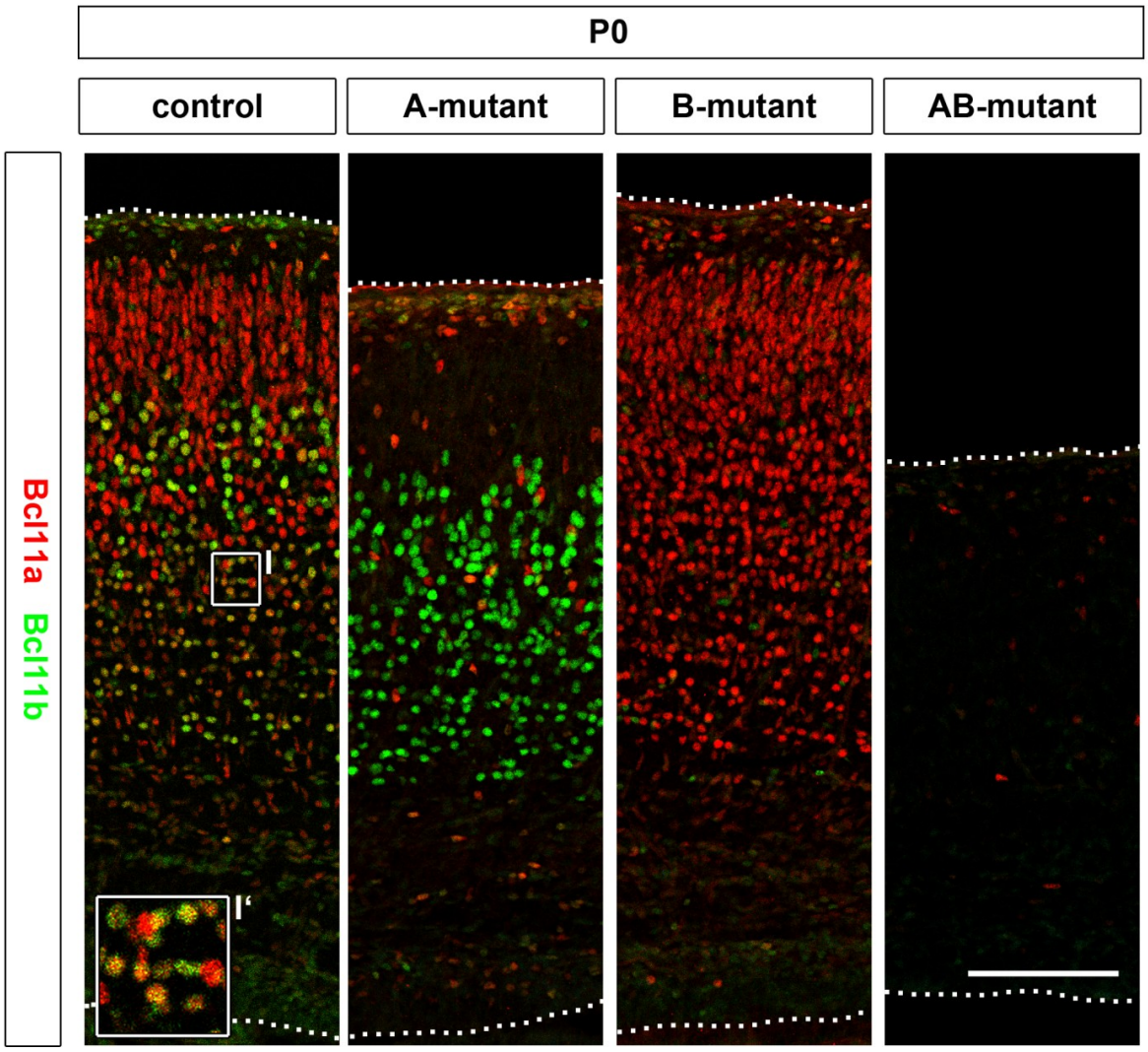


Figure 6: **Bcl11a and Bcl11b are efficiently deleted in AB-mutants at P0**

Immunohistochemistry using antibodies against Bcl11a (B-cell lymphoma 11a) (red), and Bcl11b (B-cell lymphoma 11b) (green) on frontal sections of neocortices. Control ($Bcl11a^{flox/+}$; $Bcl11b^{flox/+;}$ $Emx1^{Cre/+}$), A-mutant ($Bcl11a^{flox/flox}$; $Bcl11b^{flox/+;}$ $Emx1^{Cre/+}$), B-mutants ($Bcl11a^{flox/+}$; $Bcl11b^{flox/flox;}$ $Emx1^{Cre/+}$) and AB-mutant ($Bcl11a^{flox/flox}$; $Bcl11b^{flox/flox;}$ $Emx1^{Cre/+}$) brains are shown at day of birth (P0). (I') marks an enlargement of the marked box (I) in the neocortical deep-layers, where many cells co-express Bcl11a and Bcl11b to various extents (yellow). This experiment was repeated to a total of n=3, mice derived from at least two litters. Sections are shown in a qualitative manner, results were not quantified. Scale bar, 200µm.

3.2 AB-mutants show major deficits in overall neocortical architecture

As the first experiment shows an enormous reduction of cortical thickness, I analysed neocortical architecture in detail. To see whether the major cortical shrinkage leads to disturbance in cell arrangement, I prepared Nissl-stained methacrylate sections of P0 control and AB-mutant brains. In figure 7, a representative control and AB-mutant section is shown.

In controls, the typical six-layered architecture of the neocortex is traceable, while this is not possible in AB-mutant brains. The major cortical shrinkage already described in the immunohistochemistry experiment can be observed in greater detail.

In AB-mutants, upper-layer neurons – i.e. layers II to IV – appear comparable to controls, but a correlate of the deep-layers – i.e. layers V and VI – of control brains cannot be found. In the deeper half of the mutant neocortex, cell morphology and arrangement seem to be disturbed as well as overall cell density appears to be increased. This suggests major defects of neocortical deep-layer differentiation.

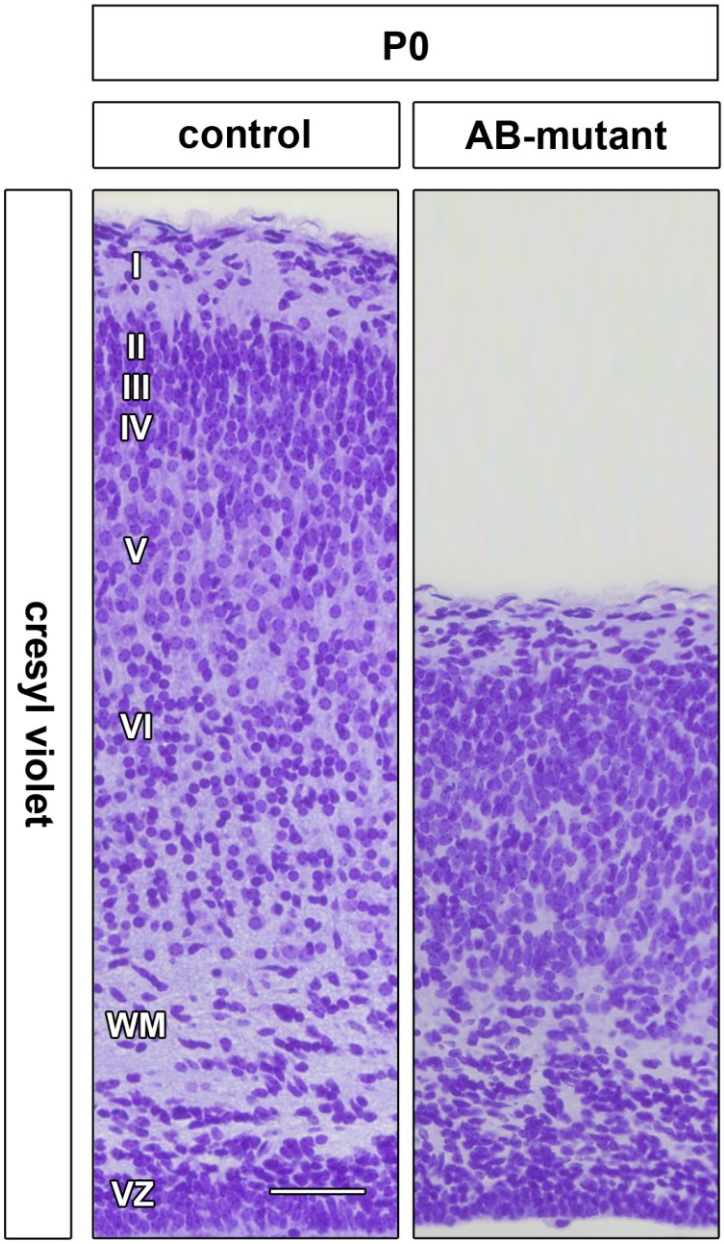


Figure 7: **AB-mutant neocortices show a major shrinkage in cortical thickness**

While AB-mutant ($Bcl11a^{flox/flox}$; $Bcl11b^{flox/flox;}$ $Emx1^{Cre/+}$) neocortical upper-layers seem to be comparable to those of a control ($Bcl11a^{flox/+}$; $Bcl11b^{flox/+;}$ $Emx1^{Cre/+}$), AB-mutant deep-layers cannot be correlated with control brains and show disturbed organization and increased cell density. Sections of 5µm thickness were analysed with cresyl violet. Analyses were made on the day of birth (P0). The typical, six-layered organization of the neocortex is noted in the control panel. This experiment was repeated to a total of n=2 litters, controls and AB-mutants were siblings. Sections are shown in a qualitative matter, results were not quantified. Scale bar, 100µm.

3.3 Neocortical deep-layer neurons show disturbance in specific marker expression at P0

As Bcl11a and Bcl11b are co-expressed in neocortical deep-layers and the histology of mutant neocortices shows strongly disturbed deep-layer architecture, expression levels of deep-layer specific transcription factors were analysed next. I prepared immunohistochemistry stainings on neocortical frontal sections of controls, A-mutants, B-mutants, and AB-mutants at P0. For my analysis I decided on three different deep-layer specific transcription factors.

Figure 8 shows the expression of Fog2 in controls, A-mutants, B-mutants and AB-mutants at P0. Transcription factor's expression in controls was set to 100% (s=6.42%), expression levels in the other genetic conditions were compared. A-mutants show a significant decrease to 72.82% (s=3.97%, $p<0.027$), B-mutants show a non-significant decrease to 82.14% (s=1.45%, $p<0.102$), while in AB-mutants Fog2 expression vanished to 3.86% (s=0.49%, $p<0.004$) compared to controls. The experiment was repeated to n=3, with brains deriving from at least two litters.

In figure 9, expression of Sox5 in controls, A-mutants, B-mutants and AB-mutants at P0 is shown. Again, expression in controls was set to 100% (s=6.21) and expression in other groups were put in comparison. A-mutants show a significant decrease to 73.98% (s=6.55%, $p<0.045$), B-mutants show a non-significant increase to 106.33% (s=2.77%, $p<0.426$) while in AB-mutants Sox5 expression significantly decreased to 4.51% (s=3.38%, $p<0.001$) compared to controls. This experiment was also repeated to n=3, brains derived from at minimum two litters.

Figure 10 shows the expression of Tbr1 in controls, A-mutants, B-mutants and AB-mutants at P0. Tbr1's expression in controls was set to 100% (s=5.74%), expression levels in the mutants were compared. A-mutants show a non-significant increase to 105.73% (s=6.15%, $p<0.533$), B-mutants show a non-significant increase to 141.13% (s=14.22%, $p<0.086$), while in AB-mutants Tbr1 expression faded to 8.87% (s=4.44%, $p<0.001$). AB-mutants show an overall weak expression of Tbr1, which was not used for quantification. Only cells expressing the transcription factor to a strong extent, typically residing in layer VI (Hevner et al., 2001 & 2002), were analysed. The experiment was repeated to a total of n=3, brains derived from at least two litters.

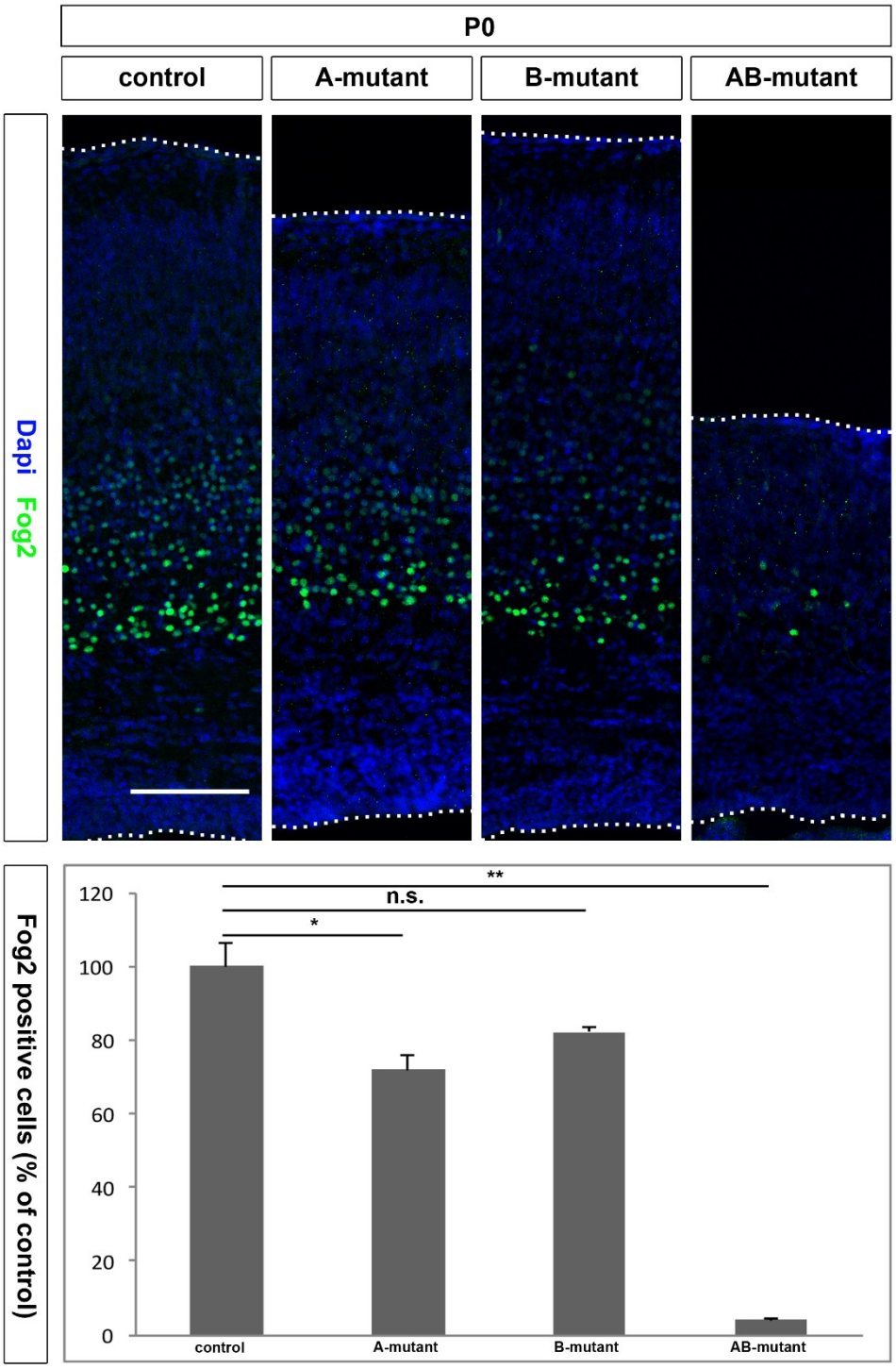


Figure 8: **Fog2, a typical neocortical marker for layer VI corticothalamic projection neurons, is severely reduced in its expression in AB-mutants**

Frontal sections of a control (Bcl11a$^{flox/+}$; Bcl11b$^{flox/+;}$ Emx1$^{Cre/+}$), A-mutant (Bcl11a$^{flox/flox}$; Bcl11b$^{flox/+;}$ Emx1$^{Cre/+}$), B-mutant (Bcl11a$^{flox/+}$; Bcl11b$^{flox/flox;}$ Emx1$^{Cre/+}$), and AB-mutant (Bcl11a$^{flox/flox}$; Bcl11b$^{flox/flox;}$ Emx1$^{Cre/+}$) neocortex at day of birth (P0). Sections were stained with antibodies against Fog2 (Friend of Gata 2) (green) and Dapi (4′,6-diamidino-2-phenylindole) (blue). Fog2 signal of the control brain is set to 100%, signals of mutants are compared. This experiment was repeated to a total of n=3, mice derived from at least two litters. Scale bar, 200µm. Graph depicts means, standard errors of the mean are shown by whiskers, *p < 0.05, **p < 0.01, n.s. = non-significant.

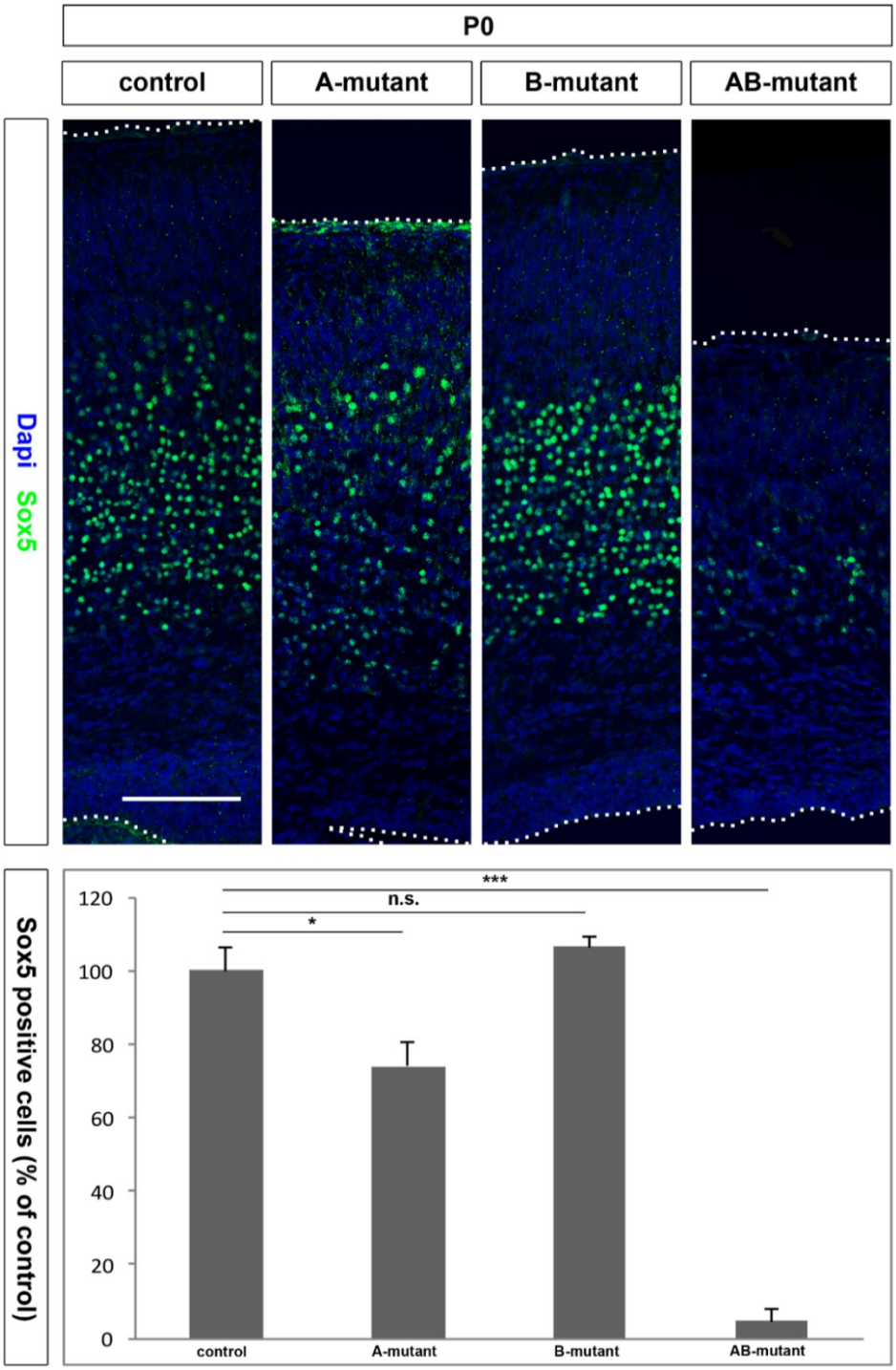


Figure 9: **The expression of Sox5, a specific marker for neocortical layers V and VI, is decreased in AB-mutants**

Frontal sections of a control ($Bcl11a^{flox/+}$; $Bcl11b^{flox/+;}$ $Emx1^{Cre/+}$), A-mutant ($Bcl11a^{flox/flox}$; $Bcl11b^{flox/+;}$ $Emx1^{Cre/+}$), B-mutant ($Bcl11a^{flox/+}$; $Bcl11b^{flox/flox;}$ $Emx1^{Cre/+}$), and AB-mutant ($Bcl11a^{flox/flox}$; $Bcl11b^{flox/flox;}$ $Emx1^{Cre/+}$) neocortex at day of birth (P0). Sections were stained with antibodies against Sox5 (Sex determining region Y box 5) (green) and Dapi (4′,6-diamidino-2-phenylindole) (blue). Sox5 signal of the control brain is set to 100%, signals of mutants are compared. This experiment was repeated to a total of n=3, mice derived from at least two litters. Scale bar, 200µm. Graph depicts means, standard errors of the mean are shown by whiskers, *$p < 0.05$, ***$p < 0.001$, n.s. = non-significant.

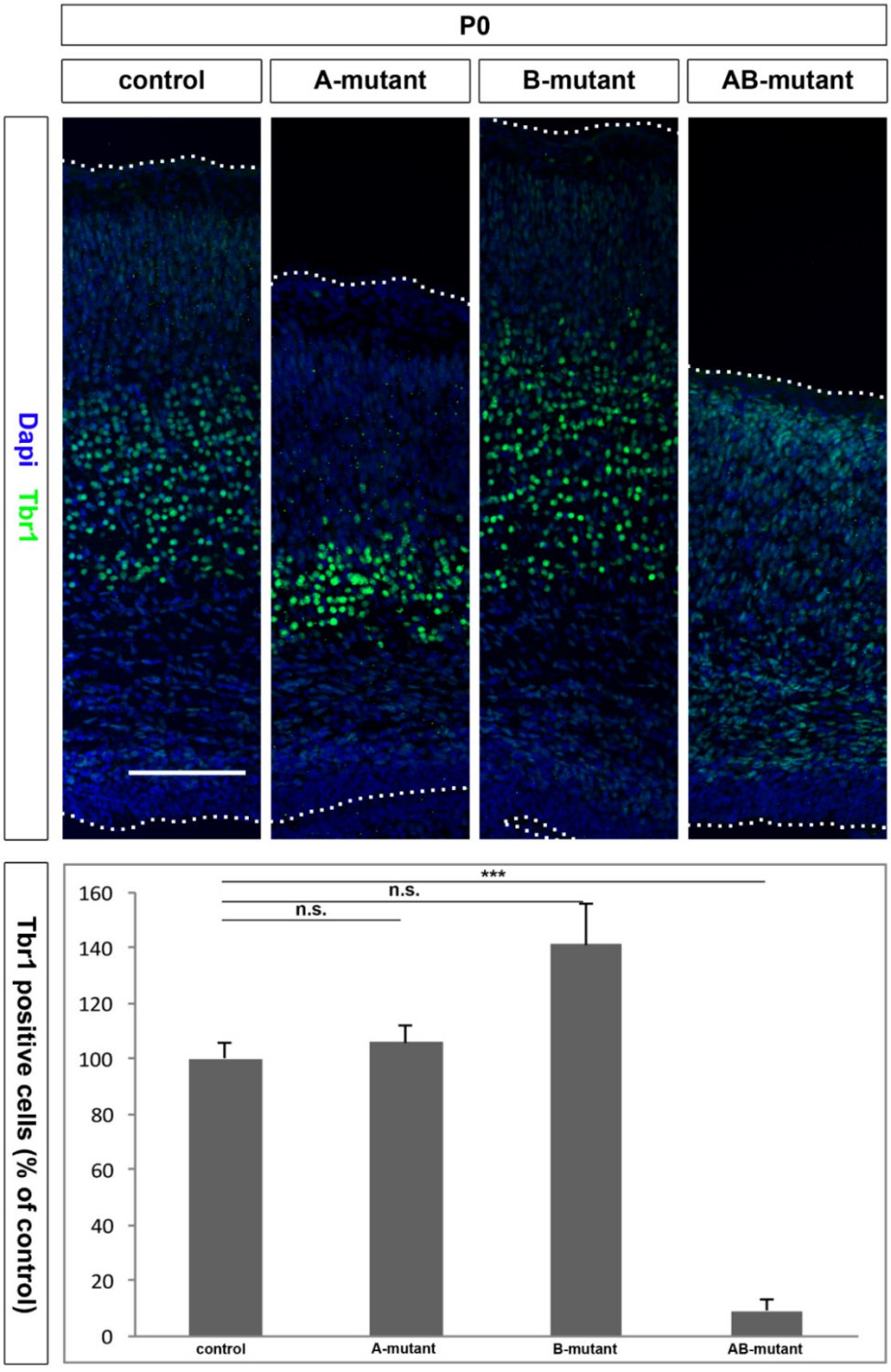


Figure 10: **Tbr1, a typical layer VI marker, is reduced in its deep-layer typical strong expression**

Frontal sections of a control (Bcl11a$^{flox/+}$; Bcl11b$^{flox/+;}$ Emx1$^{Cre/+}$), A-mutant (Bcl11a$^{flox/flox}$; Bcl11b$^{flox/+;}$ Emx1$^{Cre/+}$), B-mutant (Bcl11a$^{flox/+}$; Bcl11b$^{flox/flox;}$ Emx1$^{Cre/+}$), and AB-mutant (Bcl11a$^{flox/flox}$; Bcl11b$^{flox/flox;}$ Emx1$^{Cre/+}$) neocortex at day of birth (P0). Sections were stained with antibodies against Tbr1 (T-box brain 1) (green) and Dapi (4′,6-diamidino-2-phenylindole) (blue). Tbr1 signal of the control brain is set to 100%, signals of mutants are compared. Note the overall increase of weak Tbr1 expression in AB-mutants. This experiment was repeated to a total of n=3, mice derived from at least two litters. Scale bar, 200µm. Graph depicts means, standard errors of the mean are shown by whiskers, ***$p < 0.001$, n.s. = non-significant.

In each case, expression levels of deep-layer specific transcription factors show typical profiles in control brains as described in literature (Galazo et al., 2016; Kwan et al., 2008; McKenna et al., 2011).

In summary, deep-layer neurons of AB-mutant brains fail to express different deep-layer specific markers at P0. This phenotype could be caused by the following circumstances: (1) Deep-layer marker expressing cells are not born correctly. (2) Deep-layer-marker expressing cells die during neocortical development, or (3) neurons are born correctly, do not die, but fail to specify in a correct manner, hence do not show specific marker expression. The next experiments were executed to check for these different causes.

3.4 Neurogenesis in AB-mutant brains is unchanged

To see whether a deficit in neurogenesis leads to loss of marker expression at P0, I investigated neurogenesis at times where deep-layer specific neurons are normally born, i.e. at E11.5, E12.5 and E13.5 (Woodworth et al., 2012).

At each stage, signal of BrdU-positive cells in controls was set to 100%, signal in AB-mutants was compared. I could not detect significant changes in neurogenesis: BrdU positive cells show a non-significant decrease from 100% (s=7.62%) to 98.01% (s=8.5%, p<0.87) at E11.5, a non-significant decrease from 100% (s=4.68%) to 97.54% (s=7.57%, p<0.798) at E12.5, and a non-significant decrease from 100% (s=5.99%) to 94.34% (s=3.53%, p<0.472) at E13.5 (see figure 11).

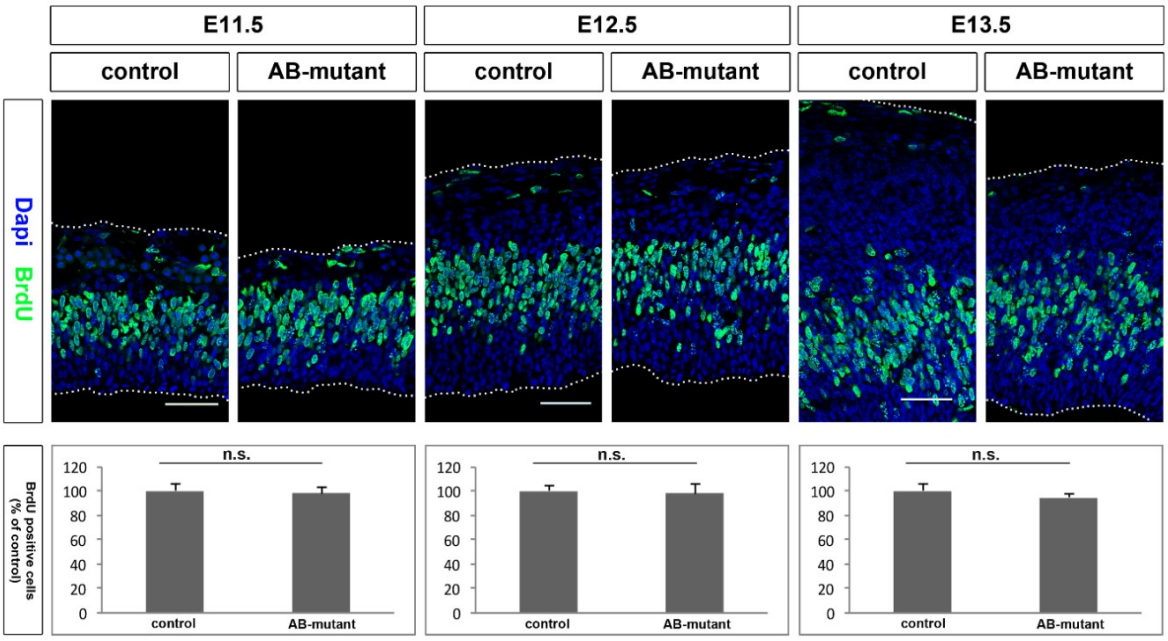


Figure 11: **Neurogenesis at early stages of AB-mutants is not impaired compared to controls**
Comparison of neurogenesis of control (Bcl11a$^{flox/+}$; Bcl11b$^{flox/+;}$ Emx1$^{Cre/+}$) and AB-mutant (Bcl11a$^{flox/flox}$; Bcl11b$^{flox/flox;}$ Emx1$^{Cre/+}$) brain at different points of neocortical development (E11.5, E12.5 and E13.5). Frontal sections of 12µm thickness were stained with Dapi (4′,6-diamidino-2-phenylindole) (blue) and antibodies against BrdU (Bromodeoxyuridine) (green). At each stage, BrdU signal of the control is 100%, signal of the AB-mutant is compared. Experiments were repeated to a total of n=3 for each date, controls and AB-mutants were siblings and were taken from at least 2 litters. Scale bars, 50µm. Graph depicts means, standard errors of the mean are shown by whiskers, n.s. = non-significant.

These experiments show that there is no significant change in BrdU-expressing cells, thus indicating no difference in generation of neurons at deep-layer specific dates of birth.

3.5 Increased cell death in embryonic stages of AB-mutant brains

To verify whether loss of P0 marker expression is due to deep-layer neurons being born correctly but dying afterwards, cleaved caspase 3 signal levels at different embryonic stages were analysed. To quantify result, absolute cleaved caspase 3 positive cell numbers were used.

At E11.5 cleaved caspase 3 signal shows a non-significant increase from 1.83 (s=0.65) in controls to 2.27 (s=0.494, p<0.618) in AB-mutants. At E12.5 a significant increase from 1.83 (s=0.333) to 3.41 (s=0.22, p<0.022), and at E13.5 a significant increase from 1.33 (s=0.22) to 3.5 (s=0.5, p<0.034) is found. At later embryonic stages, there is no significant alteration of cleaved caspase 3 signal: signal is decreased not significantly from 2.44 (s=0.53) to 1.67 (s=0.6, p<0.389) at E15.5, and also not significantly decreased from 1.83 (s=0.464) to 1.53 (s=0.462, p<0.666) at E17.5. At P0, a massive increase from 2.08 (s=0.083) to 9.42 (s=0.507, p<0.004) is observed (see figure 12).

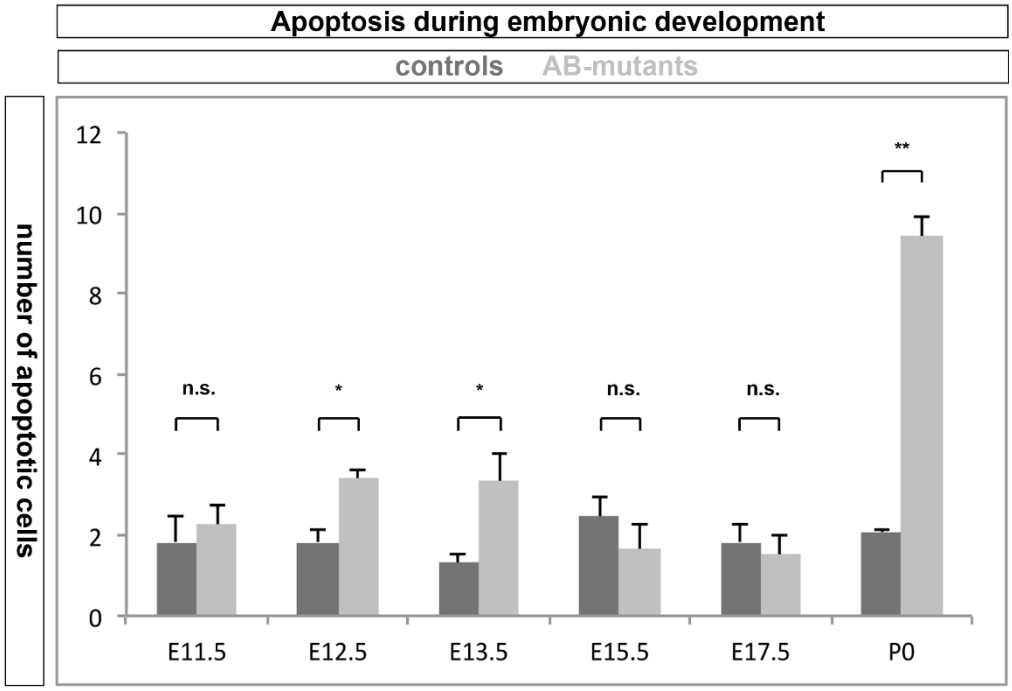


Figure 12: **AB-mutants show slight increase of apoptosis on E12.5 and E13.5, and a massive increase of apoptosis at P0**

Number of apoptotic cells of controls (Bcl11a$^{flox/+}$; Bcl11b$^{flox/+;}$ Emx1$^{Cre/+}$) (dark grey) and AB-mutants (Bcl11a$^{flox/flox}$; Bcl11b$^{flox/flox;}$ Emx1$^{Cre/+}$) (light grey). On various embryonic stages (i.e. E12.5 or E13.5) and the day of birth (P0), AB-mutants were compared to controls. Experiments were repeated to a total of n=3 for each date, controls and AB-mutants were siblings and were taken from at least 2 litters. Graph depicts means, standard errors of the mean are shown by whiskers, *p < 0.05, **p < 0.01, n.s. = non-significant.

In summary, there is a 2 fold increase of apoptotic cells at E12.5 and E13.5, which both correspond to specific dates of birth for deep-layer neurons. At P0, a 4.5 fold increase in cell death is observed. At other stages, there is no significant alteration in apoptosis signal.

3.6 Expression of deep-layer specific markers is severely reduced over neocortical development

As my previous experiments showed, cells are born in a correct manner, and some of them die during embryonic development. To check whether the missing deep-layer specific marker expression is due to mis-differentiation, animals were analysed for deep-layer specific markers at different embryonic stages. To see if deep-layer neurons differentiate at all, I checked for specific marker expression on timepoints when deep-layer neurons are born, i.e. E11.5, E12.5 and E13.5. To check whether correctly differentiated cells lose their specific marker profile, I chose E15.5 as an intermediate and E17.5 as a late state of embryonic development.

Owing to the amount of brains needed, I simplified my analyses on controls and AB-mutants, leaving A-mutants or B-mutants aside. At each point of analysis, signal in controls was set to 100%, marker expression in AB-mutants was compared.

Fog2 is a deep-layer specific transcription factor residing in layer VI. Fog2 expression should first be detectable at E12.5. This was the case in controls, but AB-mutants failed to express a significant amount of Fog2 positive cells. Analysis of later stages show that Fog2-positive cells barely form during embryonic development.

Fog2 expression at E12.5 shows a significant decrease from 100% (s=8.82%) to 14.49% (s=5.34%, $p<0.003$), at E13.5 a significant decrease from 100% (s=6.0%) to 21.0% (s=3.17%, $p<0.002$), at E15.5 a significant decrease from 100% (s=10.45%) to 2.84% (s=0.84%, $p<0.011$), and at E17.5 a significant decrease from 100% (s=7.86%) to 3.98% (s=0.36%, $p<0.007$). P0 expression was mentioned before and is shown for comparison.

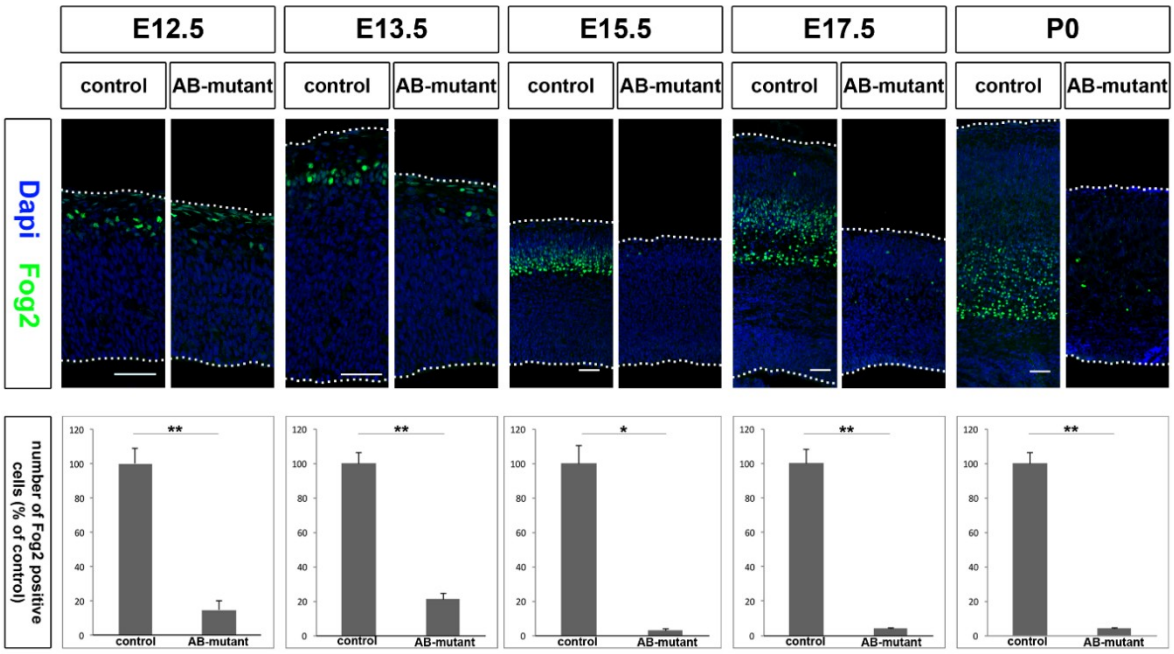


Figure 13: **Over different embryonic stages, Fog2 expression is reduced in AB-mutants**

Analysis of Fog2 (Friend of Gata 2) over embryonic stages E12.5 to E17.5 and day of birth (P0). 12µm slices were stained with Dapi (4′,6-diamidino-2-phenylindole) (blue) and antibodies against Fog2 (green). On each date, the neocortex of an AB-mutant ($Bcl11a^{flox/flox}$; $Bcl11b^{flox/flox;}$ $Emx1^{Cre/+}$), is compared to a control ($Bcl11a^{flox/+}$; $Bcl11b^{flox/+;}$ $Emx1^{Cre/+}$). At each stage, Fog2 signal of the control brain is set to 100%, signal of the AB-mutant brain is compared. Experiments were repeated to a total of n=3 for each date, controls and AB-mutants were siblings and taken from at least 2 litters. Scale bars, 100µm. Graph depicts means, standard errors of the mean are shown by whiskers, *p < 0.05, **p < 0.01.

Sox5 resides in the deep-layers V and VI and should first be detectable between E12.5 and E13.5. In the controls, signal is observed at E13.5, but again AB-mutants fail to express Sox5. Later stages show that Sox5 is not expressed during embryonic development.

Sox5 expression at E13.5 shows a significant decrease from 100% (s=4.45%) to 4.63% (s=2.43%, $p<0.001$), at E15.5 a significant decrease from 100% (s=15.33%) to 3.2% (s=0.97%, $p<0.024$), and at E17.5 a significant decrease from 100% (s=3.79%) to 0.88% (s=0.22%, $p<0.002$). P0 expression was already mentioned and is shown for comparison.

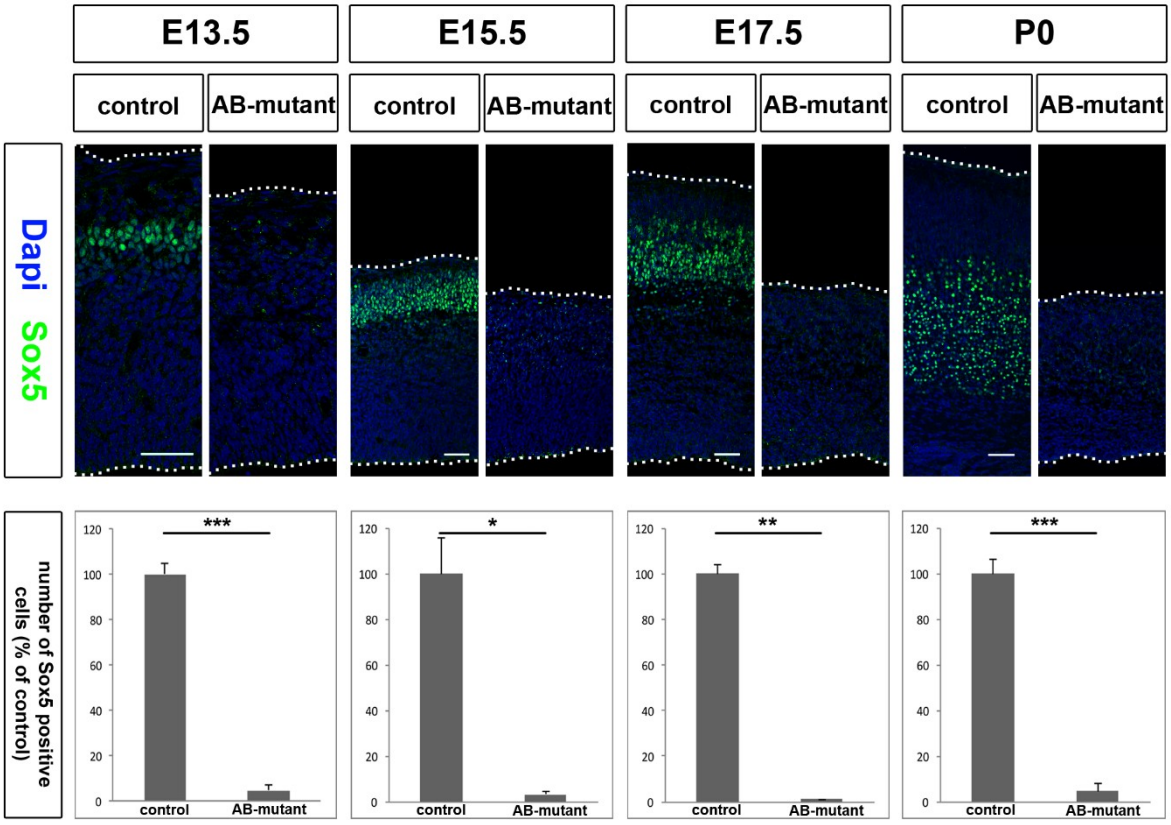


Figure 14: **Sox5 expression is reduced severely in developing AB-mutant brains**

Analysis of Sox5 (Sex determining region Y box 5) over embryonic stages E13.5 to E17.5 and day of birth (P0). 12µm slices were stained with Dapi (4′,6-diamidino-2-phenylindole) (blue) and antibodies against Sox5 (green). On each date, the neocortex of an AB-mutant ($Bcl11a^{flox/flox}$; $Bcl11b^{flox/flox;}$ $Emx1^{Cre/+}$), is compared to a control ($Bcl11a^{flox/+}$; $Bcl11b^{flox/+;}$ $Emx1^{Cre/+}$). At each stage, Sox5 signal of the control brain is set to 100%, signal of the AB-mutant brain is compared. Experiments were repeated to a total of n=3 for each date, controls and AB-mutants were siblings and taken from at least 2 litters. Scale bars, 100µm. Graph depicts means, standard errors of the mean are shown by whiskers, *$p < 0.05$, **$p < 0.01$, ***$p < 0.001$.

Tbr1 has a more complicated expression pattern in control brains: According to Hevner et al. (2001), all neurons undergo a state of low Tbr1 expression during development, which is replaced later on by expression of the final layer-specific marker, if cells specify correctly. The deep-layer specific Tbr1 high expression starts at about E13.5 and can be distinguished from the low expression.

The phenomenon of neurons undergoing low Tbr1 expression is seen in controls and AB-mutants alike until E12.5. While in controls, neurons switch their expression levels to the deep-layer specific strong expression, AB-mutant neurons retain low Tbr1 expression and fail to develop deep-layer specific signal. Remarkably, weak Tbr1 signal of AB-mutant brains expressed throughout layers II to VI does not perish during development, but is retained to postnatal stages.

Tbr1 expression at E11.5 shows a non-significant increase from 100% (s=2.79%) to 104.1% (s=11.83%, $p<0.765$) and at E12.5 a non-significant increase from 100% (s=11.68%) to 117,85% (s=19.74%, $p<0.489$). At E13.5 a significant decrease from 100% (s=15.32%) to 27.63% (s=7.61, $p<0.025$) is observed. At E15.5 a significant decrease from 100% (s=9.02%) to 12.09% (s=5.77%, $p<0.003$), and at E17.5 a significant decrease from 100% (s= 8.06%) to 1.06% (s=0.27%, $p<0.007$) is found. P0 expression was already mentioned and is shown for comparison.

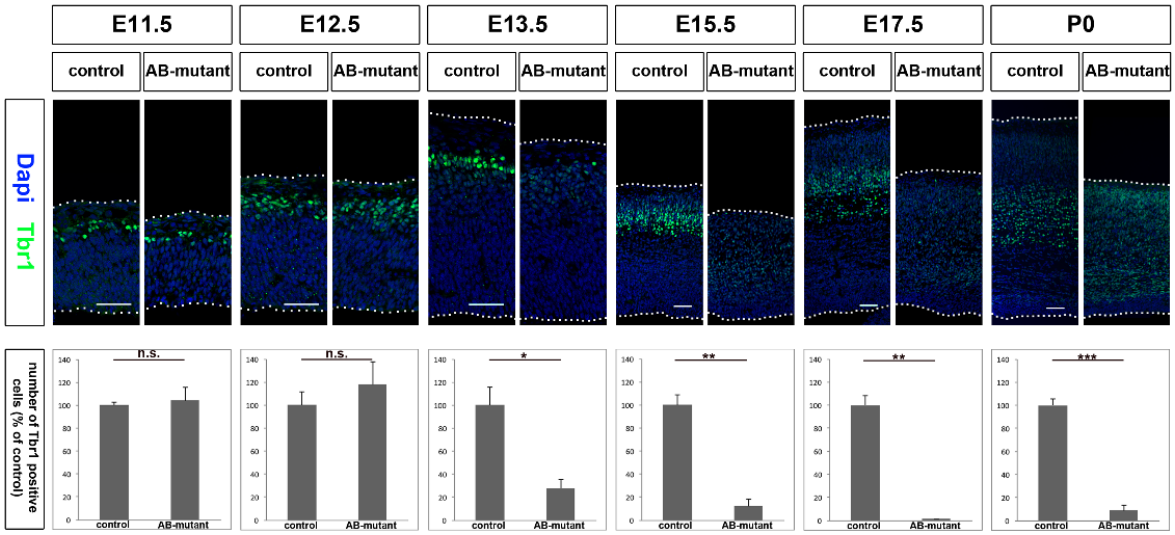


Figure 15: **Strong, deep-layer typical Tbr1 expression does not appear in AB-mutants, instead overall weak expression is retained throughout the neocortex**

Analysis of Tbr1 (T-box brain 1) over embryonic stages E11.5 to E17.5 and day of birth (P0). 12µm slices were stained with Dapi (4′,6-diamidino-2-phenylindole) (blue) and antibodies against Tbr1 (green). On each date, the neocortex of an AB-mutant (Bcl11a$^{flox/flox}$; Bcl11b$^{flox/flox;}$ Emx1$^{Cre/+}$), is compared to a control (Bcl11a$^{flox/+}$; Bcl11b$^{flox/+;}$ Emx1$^{Cre/+}$). At each stage, Strong Tbr1 signal of the control brain is set to 100%, signal of the AB-mutant brain is compared. Experiments were repeated to a total of n=3 for each date, controls and AB-mutants were siblings and taken from at least 2 litters. Scale bars, 100µm. Graph depicts means, standard errors of the mean are shown by whiskers, *p < 0.05, **p < 0.01, ***p < 0.001, n.s. = non-significant.

To summarize: Cells born on specific dates of birth of neocortical deep-layer neurons, i.e. E11.5, E12.5 and E13.5, fail to express deep-layer specific markers at any stage of neocortical development.

3.7 Cell-autonomous knockout of Bcl11a and Bcl11b

The last set of experiments was done to examine whether the changes seen in AB-mutants also occur on a cell-autonomous level. This question was approached using the *in utero* electroporation technique.

In the control condition, Bcl11a//b$^{flox/flox}$ brains were transfected with vectors containing green fluorescent protein (GFP) (annotated IRES-GFP). In mutant conditions, Bcl11a//b$^{flox/flox}$ brains were transfected with vectors containing GFP and a Cre-recombinase (annotated Cre-IRES-GFP). The co-electroporation of fluorescent protein allowed to distinguish background cells versus transfected neurons that express GFP and Cre in mutants, or only GFP in controls, respectively.

Animals were treated at E12.5 and harvested at P0. Deep-layers were identified with stainings e.g. Bcl11b, marking the upper end of layer V. Experiments were repeated to n=3. Controls and mutants were generated in equivalent experiments with mice deriving from at least two litters.

3.7.1 *In utero* electroporation of Cre effectively deletes Bcl11a and Bcl11b expression in Bcl11a//b$^{flox/flox}$ neurons

The first part of this set of experiments was executed to check if the knockout construct works on a cellular level. As shown in figure 16, Bcl11a//b$^{flox/flox}$ brains transfected with the empty vector (IRES-GFP, which corresponds to controls) manifest normal distribution of Bcl11a and Bcl11b. Co-expression of Bcl11a, Bcl11b and GFP is shown (whitish cells marked with arrows).

Transfection with Cre (Cre-IRES-GFP, which corresponds to mutants) results in almost no signal of Bcl11a or Bcl11b in transfected cells. No co-expression between GFP and Bcl11a or Bcl11b, respectively, is observed proving the knockout method to be highly efficient. Results are shown in a qualitative manner and were not quantified.

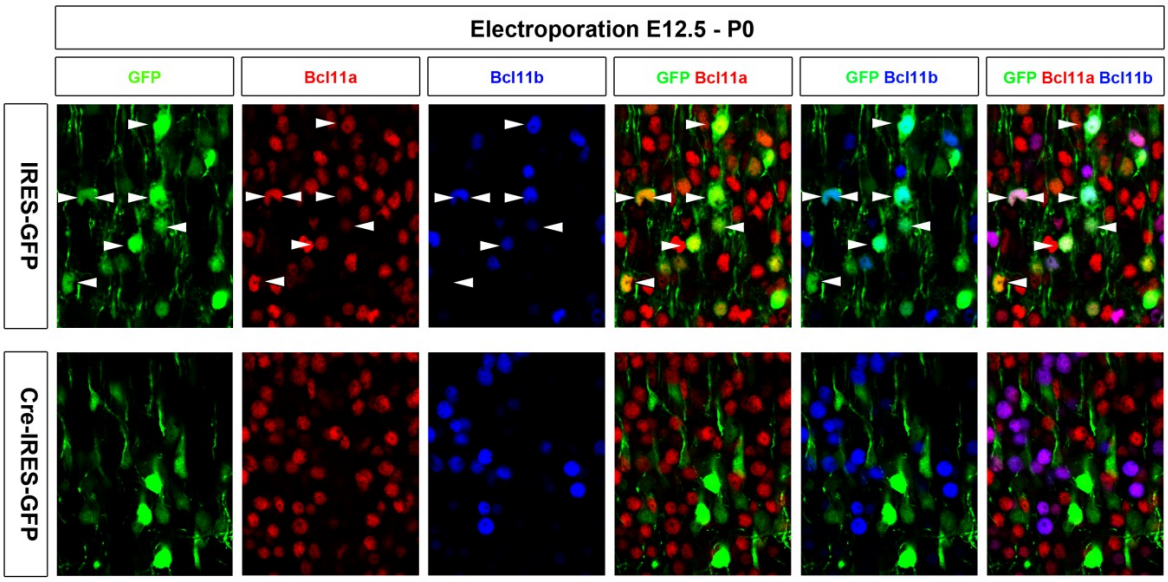


Figure 16: **Bcl11a and Bcl11b are knocked out efficiently in Bcl11a//b$^{flox/flox}$ neurons that have been transfected with Cre and GFP**

Immunohistochemistry of *in utero* electroporated Bcl11a//b$^{flox/flox}$ brains. Cells transfected with IRES-GFP express GFP (green fluorescent protein) and co-express Bcl11a (B-cell lymphoma 11a) and Bcl11b (B-cell lymphoma 11b), respectively (see arrows). Cells transfected with GFP and Cre-recombinase (Cre-IRES-GFP) lose the ability to express either Bcl11a or Bcl11b, thus do not show co-expression with GFP. Arrows mark cells expressing GFP, Bcl11a and Bcl11b. This experiment was repeated to a total of n=3, controls and mutants were generated in equivalent experiments and derived from at least two litters.

3.7.2 *In utero* electroporation of Cre leads to loss of expression of deep-layer specific markers in Bcl11a//b$^{flox/flox}$ neurons

Deep-layer specific marker expression on cell-autonomous level was investigated next. Embryos were transfected with the described vector constructs at E12.5, and sections were analysed for deep-layer markers after harvest at P0. To determine correct orientation of analysis, slides were co-stained against e.g. Bcl11b. This way, layer V (showing a strong Bcl11b signal), layer VI (residing under the strong Bcl11b signal), and upper layers (residing above the strong Bcl11b signal) could be distinguished. If marker expression in the non-electroporated cells allowed exact layering, co-staining was not necessary.

At first, cells expressing GFP, thus having been transfected, were counted in a radial unit in the respective layers. Next, all neurons expressing GFP and the deep-layer transcription factor were compared to all GFP positive cells. This was done on control and mutant conditions alike.

In the left column, figure 17 shows a significant decrease of Fog2 co-expression in all layer VI GFP positive cells from 36.63% (s=5.9%) when electroporated with IRES-GFP, to 2.06% (s=0.43%, $p<0.001$) when electroporated with Cre-IRES-GFP.

In the middle column, a significant decrease of Sox5 co-expression in layers V and VI GFP positive cells from 48.07% (s=1.05%) when electroporated with IRES-GFP, to 5.78% (s=0.75%, $p<0.001$) when electroporated with Cre-IRES-GFP, is shown.

In the right column, one can observe a significant decrease of GFP and Tbr1 co-expression in the Tbr1 high expressing zone from 66.50% (s=9.7%) when electroporated with IRES-GFP, to 9.29% (s=2.43%, $p<0.001$) when electroporated with Cre-IRES-GFP. Only cells expressing Tbr1 strongly were quantified.

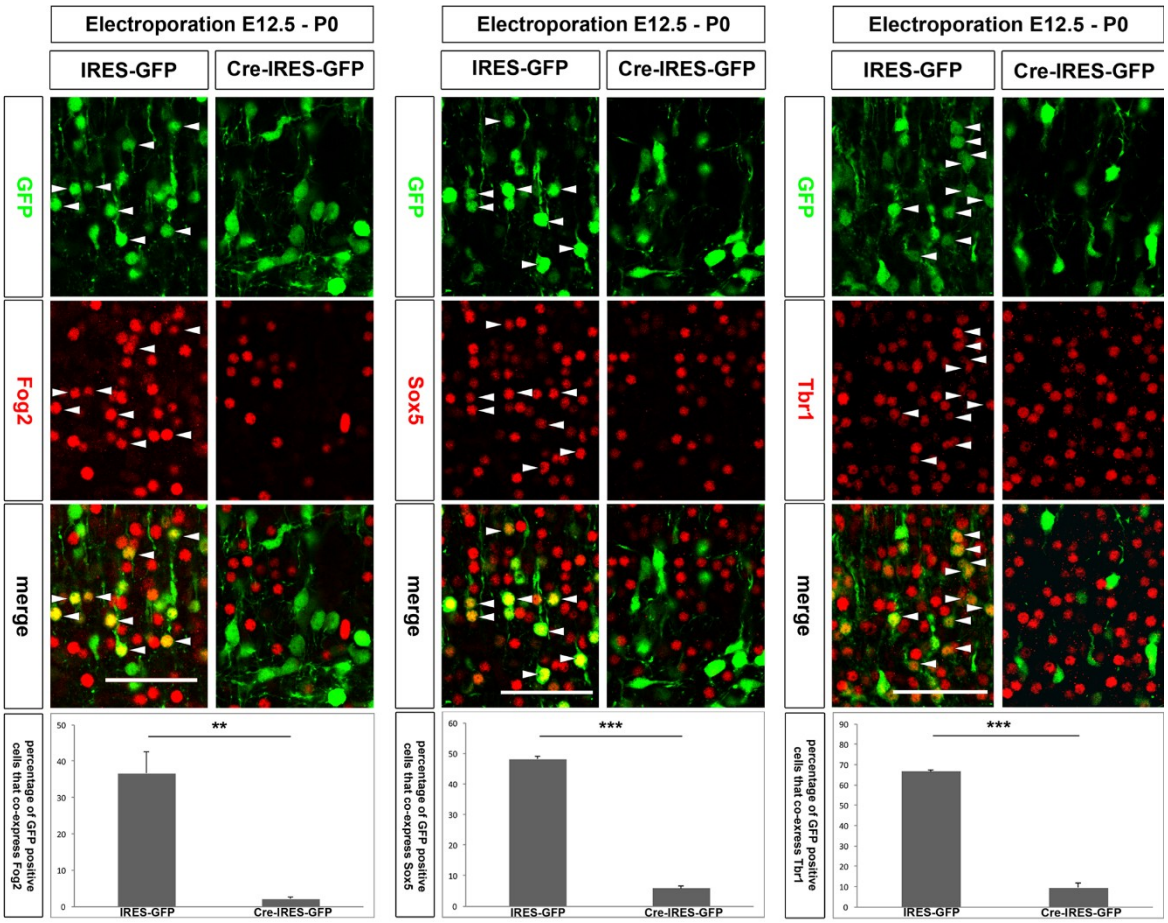


Figure 17: **In AB-mutant neurons, deep-layer specific markers are decreased on a cell-autonomous level**

While cells in the control experiment (IRES-GFP) show normal expression of deep-layer specific markers, mutated cells (Cre-IRES-GFP) fail to express these transcription factors (Fog2 (Friend of Gata 2) left column, Sox5 (Sex determining region Y box 5) middle column, Tbr1 (T-box brain 1) right column). 12µm slices were stained with antibodies against GFP (green fluorescent protein) (green) and deep-layer markers (red). Graphs show percentage of GFP-expressing cells that co-express deep-layer markers in control and mutant condition. Brains were electroporated on embryonic day 12 (E12.5) and analysed at day of birth (P0). Arrows mark cells expressing GFP and deep-layer specific transcription factors. Experiments were repeated to a total of n=3, controls and mutants were generated in equivalent experiments. Scale bars, 50µm. Graph depicts means, standard errors of the mean are shown by whiskers, **p < 0.01, ***p < 0.001.

These experiments show that deep-layer neurons lose the ability to express deep-layer specific markers on a cell-autonomous level if Bcl11a and Bcl11b are deleted.

3.7.3 Unchanged apoptosis levels in AB-mutant neurons

To check whether AB-knockout causes apoptosis on a cell-autonomous level, brains were treated as described before and analysed for cleaved caspase 3 signal. Figure 18 shows a non-significant reduction of cells that express cleaved caspase 3 and co-express GFP from 3.33% (s=13.6%) when electroporated with IRES-GFP, to 0.0% (s=0.0%, p<0.092), when electroporated with Cre-IRES-GFP.

This experiment shows that cell death does not occur on a cell-autonomous level in AB-mutant neurons.

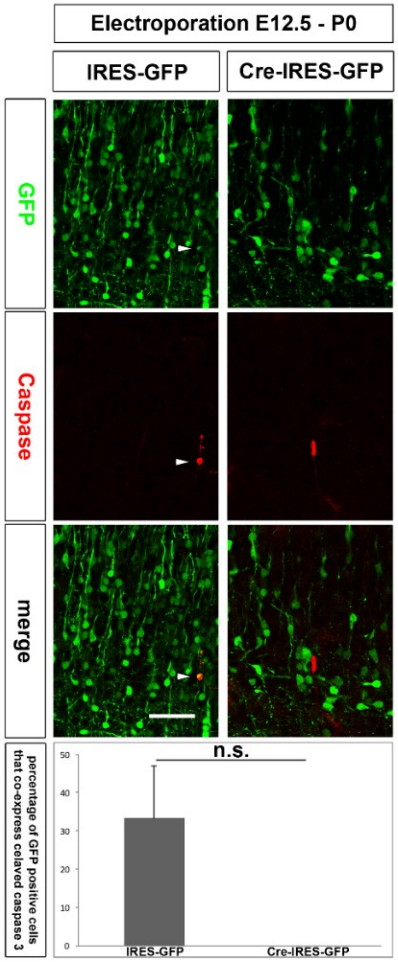


Figure 18: **No apparent difference of cleaved caspase 3 signal in control and mutant brains**
12µm frontal sections of neocortices of control condition (IRES-GFP) or mutant condition (Cre-IRES-GFP) were stained with antibodies against GFP (green fluorescent protein) (green) and analysed for caspase (cleaved caspase 3) (red). Graphs shows percentage of cleaved caspase 3 positive cells that co-express GFP in control and mutant condition. Brains were electroporated on embryonic day 12 (E12.5) and analysed at day of birth (P0). Arrow marks positive cell. These experiments were repeated to a total of n=3, controls and mutants were generated in equivalent experiments. Scale bar, 100µm. Graph depicts means, standard errors of the mean are shown by whiskers, n.s. = non-significant.

3.7.4 Increased expression of upper-layer markers in AB-mutant neurons

The last experiments were done to see if more upper-layer specific markers are expressed in deep-layer neurons, as these cells may undergo a fate-switch from deep- to upper-layer neurons. For these experiments, Cux1 and Brn2 as typical upper-layer markers were chosen.

In the region of interest, all cells expressing GFP were counted. Afterwards, cells co-expressing GFP and upper-layer markers were counted and compared. This was done on control and mutant conditions alike.

Figure 19 shows Cux1 co-expression on GFP positive cells (left column) counted in layer VI, which is significantly increased from 1.81% (s=0.62%) when electroporated with IRES-GFP, to 32.03% (s=4.0%, $p<0.005$) when electroporated with Cre-IRES-GFP. Brn2 co-expression signal (right column) counted in the Tbr1 high signal zone is significantly increased from 25.52% (s=4.07%) when electroporated with IRES-GFP, to 58.47% (s=2.8%, $p<0.001$) when electroporated with Cre-IRES-GFP.

Taken together with previous findings, these experiments show that AB-mutant neurons residing in neocortical deep-layers fail to express deep-layer specific markers, but fail upper-layer specific markers instead.

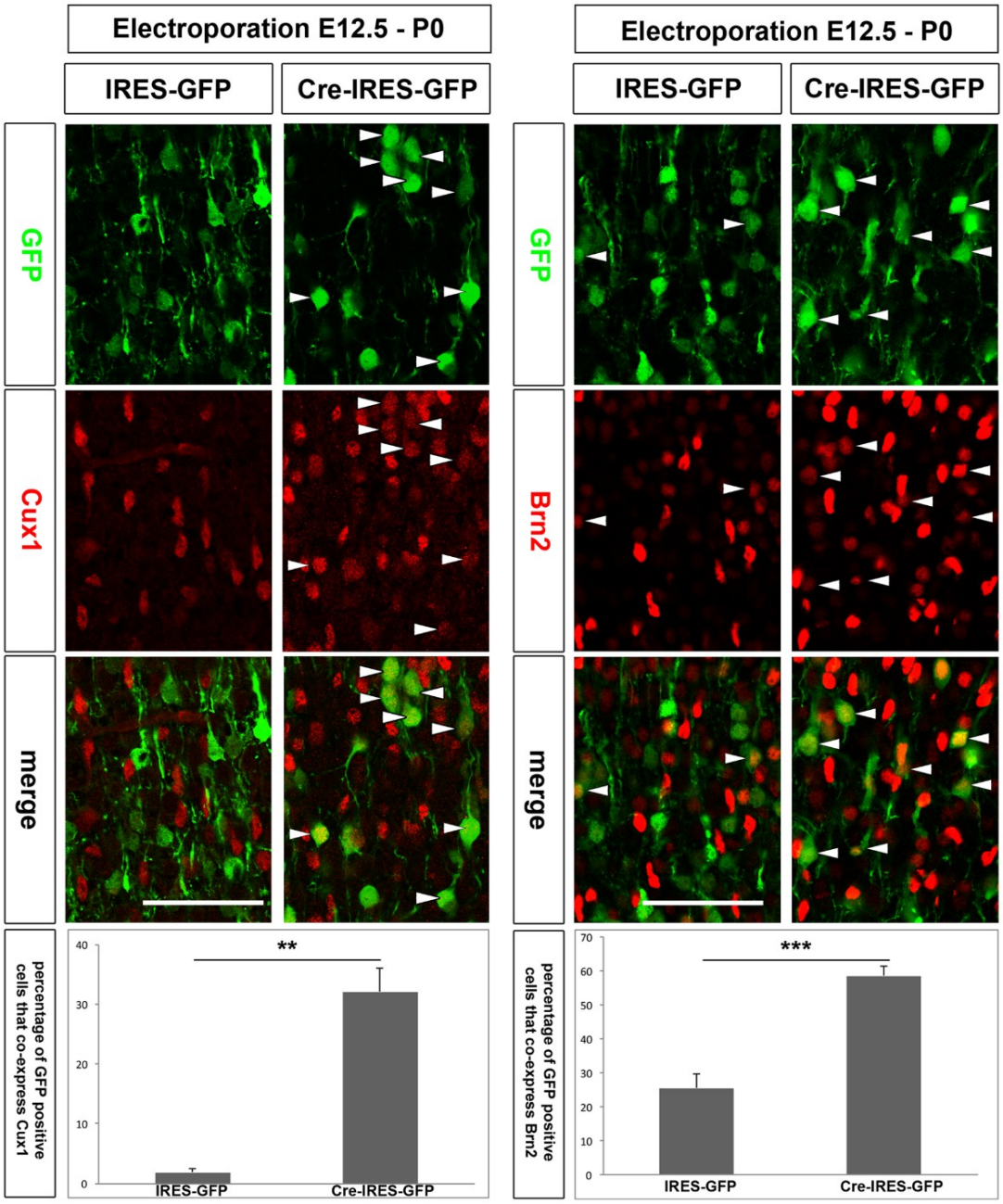


Figure 19: **Alterations of upper-layer markers in brains electroporated with Cre-IRES-GFP**

While cells in the control experiment (IRES-GFP) show normal expression of upper-layer specific markers, mutated cells (Cre-IRES-GFP) over-express these transcription factors in neocortical deep layers (Cux1 (cut like homeobox 1) left column, Brn2 (Brain 2) right column. 12µm slices were stained with antibodies against GFP (green fluorescent protein) (green) and upper-layer markers (red). Graphs show percentage of GFP-expressing cells that co-express upper-layer markers in control and mutant condition. Brains were electroporated on embryonic day 12 (E12.5) and analysed at day of birth (P0). Arrows mark cells expressing GFP and upper-layer specific transcription factors. Experiments were repeated to a total of n=3, controls and mutants were generated in equivalent experiments. Scale bars, 50µm. Graph depicts means, standard errors of the mean are shown by whiskers, **$p < 0.01$, ***$p < 0.001$.

4.0 Discussion

In this study, I investigated the phenotype of Bcl11a$^{-/-}$; Bcl11b$^{-/-}$ double-knockout mice. Bcl11a and Bcl11b are two highly related zinc-finger transcription factors that both share functions in the neocortex and are expressed in similar regions of the brain, e.g. the deep neocortical layers V and VI. Further, I searched for possible compensatory interactions of these two transcription factors by comparing double-knockouts to mice only lacking either Bcl11a or Bcl11b.

4.1 Neocortical morphology

The neocortex is organised in a distinct, six-layered structure. Each layer executes specific tasks. The six neocortical layers are orientated parallel to the ventricular surfaces and vary in thickness regarding brain areas, e.g. layers V and VI are increased in somatomotoric and decreased in somatosensory parts of the neocortex.

At P0, AB-mutant neocortices show a major shrinkage in overall neocortical thickness. The typical, six-layered architecture cannot be retraced anymore and in the white matter, cell density seems to be increased (see figure 7). Upper layers look comparable to controls, while this is not the case regarding neocortical deep-layers.

A-mutants show a minor shrinkage in neocortical thickness, as it has been described in literature (Wiegreffe et al., 2015). B-mutants do not manifest an apparent shrinkage in overall neocortical thickness. Interestingly, loss of neocortical thickness is by far greater in double-knockout mice, than in the phenotype of either Bcl11a or Bcl11b knockout mice combined.

This finding suggests possible compensatory interactions between the two transcription factors: In A-mutants, Bcl11b compensates the loss of Bcl11a at least partially, and only a small loss of neocortical thickness is observed. In B-mutants, loss of the transcription factor does not lead to thickness-reduction at all. If Bcl11a and Bcl11b are deleted simultaneously, no transcription factor can compensate losses and cortical thickness is impaired severely.

Analyses of neocortical morphology suggest the knockout affects deep-layers the strongest. Experiments examining expression patterns of Bcl11a and Bcl11b show that the transcription factors are largely co-expressed in neocortical deep-layers and this co-expression is lost upon double-knockout (see figure 6).

The neocortical deep-layers show specific transcription factors that distinguish them from upper-layers. These specific transcription factors perform tasks like guiding neuronal specification or forming and maintaining deep-layer typical connections like the CST or corticothalamic projections.

At P0, three typical deep-layer specific transcription factors are almost lost completely in AB-mutants: Fog2, a specific layer VI marker that guides corticothalamic projections (Galazo et al., 2016). Sox5 that is typically expressed in layers V and VI, maintains corticothalamic projections and is important for correct specification and connectivity of neurons (Lai et al., 2008; Kwan et al., 2008). Tbr1, a transcription factor that is expressed strongly in layer VI and is important for correct layer formation and CPN projections (Hevner et al., 2001 & 2002; McKenna et al., 2011).

This nearly complete loss of deep-layer specific marker expression in double-mutants does not occur in mice lacking either Bcl11a or Bcl11b:

Compared to controls, A-mutants significantly lose Fog2 expression by 30%, while in B-mutants, Fog2 expression is not significantly decreased by 17%. In AB-mutants, Fog2 is lost significantly to 95% (see figure 8), which is clearly more than reduction of Fog2 expression in either A-mutant or B-mutant phenotype combined.

Similarly, Sox 5 is significantly decreased by 25% in A-mutants. In B-mutants a non-significant increase by 6% is observed. Double-mutants significantly lose Sox5 expression to 5% (see figure 9) compared to controls, which again is clearly more than the combination of alterations of either A- or B-mutant phenotype taken together.

Tbr1 is not significantly increased by 6% in A-mutants, and not significantly increased by about 40% in B-mutants. In AB-mutants, a significant decrease by 90% is observed (see figure 10) which is surprising, as Tbr1 expression is raised in A- and B-mutants.

According to literature, Bcl11a directly inhibits expression of Tbr1 (Cánovas et al., 2015). Knocking down Bcl11a via IUE led to a significant increase in Tbr1 expression. In my experiments, Tbr1 expression was increased in Bcl11a$^{-/-}$ animals, but not at a significant level. This contradiction to the results of Cánovas et al. (2015) could be explained by the fact that they executed *in utero* electroporation experiments whereas I analysed compound knockout mice. Woodworth et al. (2016) reported the following: Upon deletion of Bcl11a, they detect a decrease of Tbr1 by around 30%. This finding contrasts my experimental results, as well as the results of Cánovas et al. (2015).

Furthermore, Tbr1 is directly inhibited by Bcl11b (Srinivasan et al., 2012). Upon deletion of Bcl11b, the authors detect an increase of Tbr1 signal in layer V by 2.5 fold, and in layer VI by 1.3 fold. In my experiments, Tbr1 is also increased in Bcl1b$^{-/-}$ mice, but not significantly.

There is no explanation in literature, why Tbr1 signal is decreased by 90% if Bcl11a and Bcl11b are deleted. Two sources (Cánovas et al., 2015 and Srinivasan et al., 2012) report a direct inhibition of Tbr1 via Bcl11a and Bcl11b, respectively. I cannot provide an answer why Tbr1 would be absent if both direct inhibitors were to be deleted. However, according to Hevner et al. (2001), all projection neurons are undergoing a phase of weak Tbr1 expression, and at P0 a group of cells that expresses Tbr1 strongly resides in layer VI. Weak Tb1 expression is thought to indicate a state of neuronal specification, while strong Tbr1 expression is a typical marker for deep-layer neurons. In my experiments I show that weak Tbr1 expression is increased throughout the neocortex, while strong Tbr1 expression is absent in neocortical deep-layers (see figure 10). This could indicate a disturbance in correct specification of CPNs: At P0, neurons are still not specified correctly, and thus express weak Tbr1 signal, but fail to express layer VI typical strong expression. This could indicate that a combined loss of Bcl11a and Bcl11b leads to mis-specification of neurons (thus the overall weak Tbr1 signal) and furthermore inhibits expression of deep-layer typical strong Tbr1 expression.

Disturbed expression patterns of typical deep-layer markers in AB-mutants support the theory of compensation between Bcl11a and Bcl11b: At P0, only a small, often non-significant increase or decrease of deep-layer specific markers is observed in A- or B-mutants. In AB-mutants, expression levels fade to under 10% compared to controls. This indicates that the loss of Fog2 and Sox5 in Bcl11a mutants can be partially saved by Bcl11b and vice versa.

4.2 Neocortical development

The six-layered neocortex is generated in a distinct manner: Neurons emerging from stem-cell zones (SVZ/VZ) form neocortical layers. In this process, the neocortical layers are generated in an "inside-out" fashion: Early born neurons (E11.5 to E13.5) generate neocortical deep-layers VI to V, while later born neurons (E14.5 to E17.5) migrate past and generate layers IV to II.

Regarding AB-mutants, neocortical deep-layers are severely disturbed at P0. This could have multiple reasons: (1) neurons are not born correctly; (2) neurons are born correctly, but die during embryogenesis; or (3) neurons are born correctly, do not die in neocortical development but are mis-specified, hence do not express deep-layer specific markers.

Pulse-chase experiments at deep-layer specific dates of birth (i.e. E11.5, E12.5 and E13.5) show that there is no difference in neurogenesis in AB-mutants compared to controls (see figure 11). Thus, absence of deep-layer specific markers is not due to a deficit in neurogenesis.

Apoptosis analyses over neocortical development show an increase in apoptosis at E12.5 and at E13.5 about 2.5 fold. There is no significantly increased rate of apoptosis in other stages of neocortical development, except on P0 when massive cell death occurs, manifesting with increased rates of apoptosis by more than 4 fold (see figure 12).

Neurons die on deep-layer specific dates of birth, which can explain some of the loss of deep-layer specific marker signal at P0. Further, at P0, the day of deep-layer marker analysis, massive cell death occurs, which results in absence of deep-layer specific signal. Although these experiments support the thesis that loss of marker expression is due to apoptosis, I think it is unlikely that a 2.5 fold increase in apoptosis at deep-layer specific dates of birth and increased apoptosis at P0 is strong enough to decrease deep-layer specific signal to 5-10% compared to controls.

To further analyse reasons for loss of deep-layer specific expression at P0, deep-layer specific markers were analysed in their expression over neocortical development. E11.5, E12.5 and E13.5 were chosen as stages of deep-layer generation, whereas E15.5 and E17.5 were chosen as stages of later neocortical development.

Regarding Fog2, neurons fail to express this deep-layer specific marker from E12.5 onwards on. On E11.5, no signal was detectable in controls and AB-mutants (see figure 13). This overall disability to express Fog2 over time suggests that the loss of Fog2 signal at P0 is at least not solely due to P0 apoptosis. Further, I doubt that the 2 fold increase of apoptosis on E12.5 and E13.5 is high enough so all cells normally expressing Fog2 decay. This indicates that on top of cell death there is a disability of deep-layer neurons to express this deep-layer specific marker.

Analysing Sox5, neurons again fail to express this specific marker from E13.5 onwards. Prior to this point, no marker expression was detectable in controls and AB-mutants (see figure 14). Again, loss of Sox5 over neocortical development shows that P0 apoptosis cannot solely explain absence of Sox5 at P0. Again, I think it is unlikely that the E13.5 increase in apoptosis results in death of all neurons normally expressing Sox5. This suggests again that on top of cell death there is a neuronal disability to express this transcription factor.

Finally, analysing Tbr1 shows no significant decreases from E11.5 to E13.5 (see figure 15). This accords to Hevner et al. (2001) postulating all neurons undergo Tbr1 expression before activating their layer-specific markers. Loss of Tbr1 signal is observed in later stages, where strong Tbr1 signal should indicate developing deep-layers. As this loss occurs in neocortical development, P0 apoptosis once more can be ruled out to be the main cause for loss of signal at P0. Cell death on E12.5 and E13.5 will reduce the amount of deep-layer neurons, but as mentioned before can in all likelihood not result in cell death of all deep-layer neurons.

In summary, I show that loss of deep-layer marker on P0 cannot be due to massive P0 apoptosis. Further I presume that E12.5 and E13.5 apoptosis - which is only increased by about 2.5 fold - cannot result in absence of all deep-layer specific neurons. This in turn indicates a disability of deep-layer neurons to express deep-layer specific markers.

I consider cell death on E12.5 and E13.5 being due to the disability of neurons to generate their specific marker profile. As they do not express correct specification, they possibly do not receive further input from their surroundings or receive cell death signals. Massive cell death on P0 could be due to neurons disability to integrate into neuronal connectivity.

Findings from Wiegreffe et al. (2015) support this thesis at least for Bcl11a mutant neurons. The authors have shown increased apoptosis rates on P5 neurons if Bcl11a is deleted from E14.5 on, but this increase of apoptosis is not observed if Bcl11a is deleted later at E18.5. The authors discuss that the early loss of Bcl11a leads to neuronal disability of integrating in existing connectivity networks, resulting in cell death.

4.3 Cell-autonomous reactions

As a next step, I wanted to answer whether the described phenotype is due to cell-autonomous reactions. Using *in utero* electroporation, a mosaic structure was generated and analysed. Bcl11a//b$^{flox/flox}$ neurons were transfected with vectors containing GFP and Cre to generate mutated neurons on a not influenced background. In a similar experiment, neurons were only transfected with GFP to mark control neurons.

Embryos were transfected with vectors on E12.5 and harvested at P0. Brains were analysed for expression of Bcl11a and Bcl11b, as well as the deep-layer specific markers Fog2, Sox5 and Tbr1, cleaved caspase 3 and the upper-layer specific markers Brn2 and Cux1.

The first experiment showed that the cell-autonomous knockout was successful: GFP marked mutant neurons did not express Bcl1a or Bcl11b, respectively, while this was the case in the similar control experiment lacking the Cre vector (see figure 16).

Investigation of deep-layer specific marker expression showed that Fog2, Sox5 and strong Tbr1 expression is lost in over 90% of GFP marked mutated neurons on the non-influenced background (see figure 17). This suggests that neurons' disability to express deep-layer specific markers is due to intracellular mechanisms and is not the result of altered extracellular signals.

Screening for cell apoptosis did not lead to significant results (see figure 18). There were simply too few cleaved caspase 3 positive cells for statistical analyses. There was not a single cleaved caspase 3 positive cell in the group of mutated neurons. The absence of cleaved caspase 3 positive cells could be the result of mutated cells already being dead, thus not expressing signal anymore. This seems unlikely to me, as there are still numerous mutated GFP positive neurons intact and several caspase positive cells were seen on compound knockout P0 frontal sections. I suggest that there is no increase in cell death in

the mosaic experiment due to a correctly functioning background: Neurons surrounding the mutated cells establish connections and may manage to integrate the mutated neurons to some extent. In the compound knockout background, all or at least most neurons fail to form functioning connections, so cells are not integrated and undergo apoptosis.

Finally, mosaic sections were analysed for expression of upper-layer markers in neocortical deep-layers. Via marker expression (like Bcl11b or strong Tbr1 expression) deep-layers were classified and upper-layer marker expression in this region was analysed. Interestingly, deep-layer neurons express upper-layer markers at significally increased levels. Cells expressing Brn2 and Cux1 are both increased by a multiple (see figure 19).

There are two possible explanations for this finding: First, neurons fail to express deep-layer markers, and express upper-layer markers instead, thus undergoing a so-called fate-switch. Second, upper-layer neurons fail to migrate correctly and are still residing in deep-layers at P0. Wiegreffe et al. (2015) described neurons' disability of correct migration upon deletion of Bcl11a, so this could be a reasonable explanation.

It seems unlikely to me that mis-migration alone results in an increase of Cux1 positive deep-layer localised cells from 2 to 32%. This would indicate a massive shrinkage of upper-layers, as their cells reside in the wrong location. Unfortunately, this could not be addressed in my experiments.

In summary, my experiments show that mis-specification of deep-layer neurons happens on a cell-autonomous level. Further, increased apoptosis in compound mutant mice seems to be triggered by extracellular factors, as there is hardly any cell death observed in the mosaic construct. Upper-layer markers are increased in deep-layers, most likely due to both mis-migration and mis-specification of neurons.

4.4 Prospect and future studies

My study laid the mere foundation of analysing the phenotype Bcl11a and Bcl11b double-mutant mice. There are still numerous fascinating questions to answer:

What is the functional correlate of the phenotype strongly affecting neocortical deep-layers? First experiments indicate that AB-mutants do not form correct corticospinal connections, which suggests a massive functional deficit of AB-mutant brains. It has already been shown, that Bcl11b$^{-/-}$ mice do not form a functioning CST, stopping at pons level (Arlotta et al., 2005). The CST originates from layer V neurons, which are strongly affected by the double-knockout.

Layer VI is also heavily affected by the AB knockout. Tbr1 and Fog2, which should be expressed here, both have an important function in the maintenance and specification of layer VI typical projections, e.g. corticothalamic connections. (Hevner et al., 2002; Galazo et al. 2016). It would be interesting to see the correlate of the absence of specific layer VI transcription factors in corticothalamic projections.

Bcl11a and Bcl11b, respectively, enhance and inhibit other transcription factors. Srinivasan et al. (2012) postulate that Bcl11b inhibits Tbr1. Cánovas et al. (2015) state that Bcl11a directly inhibits Tbr1. Logically, if Bcl11a and Bcl11b were to be deleted, this would result in a massive increase in Tbr1. In AB-mutants, I observe the contrary: Strong Tbr1 signal is almost absent. The theories of transcription factor cascades like the ones discussed by McKenna, Srinivasan or Cánovas (McKenna et al., 2011; Srinivasan et al., 2012, Cánovas et al., 2015) do not seem to be transferable from either Bcl11a or Bcl11b mutants to AB double-mutant mice. Further experiments have to be executed to investigate for transcription factor cascades of Bcl11a and Bcl11b.

The probably most interesting part of my studies is the almost complete absence of deep-layer specific transcription factors. Not stated in literature so far, AB-mutants lose several markers that should be expressed in neocortical deep-layers. This absence in turn suggests Bcl11a and Bcl11b as master regulators of deep-layer specification. Loss of one of the factors may be coped partially by its counterpart, but double-knockout leads to mis-specified and anatomically disturbed deep-layers.

Furthermore, it looks like AB-mutants do not form a functioning CC (corpus callosum). Neuronal projections fail to cross to the other hemisphere, but form Probst-bundles instead (data not shown). It would be most interesting to understand which defects lead to this malfunctioning CC: according to literature, deletion of Satb2 - a transcription factor typical for neurons projecting to the other hemisphere and is to a big part expressed in upper-layers - results in a malfunctioning CC (Britanova et al., 2008), which looks similar to the defects I observe in AB-mutants.

Can the malfunctioning CC be traced back to a loss of Satb2? Srinivasan et al. (2012) have shown that callosal neurons lacking Satb2 are partially rescued by up-regulation of Bcl11b. It has further been shown by the same group that Satb2 inhibits Bcl11b. Britanova et al. (2008) show ectopical expression of Bcl11b in Satb2 mutated upper-layers. So Satb2 and Bcl11b seem to play the role of counterparts in the neocortex. Why does the CC of AB-mutants look similar to the one described in $Satb2^{-/-}$ mutants? Or is this finding not effected by alteration of Satb2?

A different possible explanation for the mal-formation of the corpus callosum could lie in a mis-differentiation of upper layer neurons: As I have shown in analyses regarding Tbr1, there is an increase in weak Tbr1 signal, that reaches out to the upper layers. According to Hevner et al. (2001) this weak Tbr1 expression indicates a state of not completed differentiation. Maybe upper-layer neurons are also affected by loss of Bcl11a and Bcl11b and fail to specify correctly, thus do not construct their typical projection and a mal-formation of the CC is observed.

Another interesting question is why it proved to be very difficult to harvest AB-mutant mice. P0 mutants looked physically weaker compared to their siblings, and it was not possible to trace mutants to late prenatal stages, as they tended to die soon after birth. It is known that not neocortex-restricted Bcl11b mutants die soon after birth (Arlotta et al., 2005), as mice lacking Bcl11a overall do, too (Liu et al., 2003). In either Bcl11a- or Bcl11b-mutants, using the Cre/loxP system proves efficient to generate mutants up to late postnatal stages. Why is this not possible regarding AB-mutants? Are they just weaker in struggle for survival compared to their littermates and die? I noticed that even at embryonic stages, I could not harvest nearly as many AB-mutants as it should have been the case, statistically. This indicates AB-phenotype has to be severe enough to cause death of the organism, even if restrained to the neocortex. It would be fascinating to know more about these facts.

Of course, molecular targets of AB-knockout have to be found. Which genes are directly influenced by absence of both transcription factors? Is there a molecular pathway that shows interaction of Bcl11a and Bcl11b?

The time spent on research in this field was interesting and fascinating and I am looking forward to seeing new findings about Bcl11a and Bcl11b.

5.0 Summary

In my thesis, I analysed the phenotype of Bcl11a (B-cell lymphoma 11a); Bcl11b (B-cell lymphoma 11b) compound double-mutant mice and the influence of the lost transcription factors on neocortical development.

AB-mutants ($Bcl11a^{flox/flox}$; $Bcl11b^{flox/flox}$; $Emx1^{Cre/+}$) show reduced neocortical thickness and manifest with morphologically disturbed deep-layers. Lost co-expression of Bcl11a and Bcl11b in layers V and VI further suggests neocortical deep-layers as a location strongly affected by the knockout.

At the day of birth, deep-layer specific transcription factors are hardly expressed in AB-mutants. This loss of marker expression is not due to a lack of deep-layer specific neurogenesis, but to a combination of increased apoptosis and mis-specification of deep-layer neurons during neocortical development.

Upon deletion of both Bcl11a and Bcl11b, deep-layer specific marker expression is severely reduced, although it is only influenced minorly in mice lacking either Bcl11a or Bcl11b. AB-mutants are influenced far stronger than loss of either Bcl11a or Bcl11b can explain, which in turn indicates compensatory interactions between Bcl11a and Bcl11b.

The observed phenotype of compound AB-mutant brains is verifiable in experiments focusing on cell-autonomous conditions: Mutated neurons on a not genetically modified brain background fail to express deep-layer specific transcription factors. Interestingly, neurons do not undergo massive cell death as observed in compound mutant mice. This suggests increased apoptosis is caused by extracellular mechanisms.

AB-mutated neurons in neocortical deep-layers lose the ability to express deep-layer transcription factors, but express upper-layer specific markers instead.

My study shows that Bcl11a and Bcl11b are of critical importance for specification of neocortical deep-layers. Double-knockout leads to loss of deep-layer specific transcription factors. *In utero* experiments suggest a fate switch of deep-layer neurons, now expressing upper-layer specific markers. Taken together, my results suggest Bcl11a and Bcl11b as master regulators of neocortical deep-layer specification in neocortical development and further indicate compensatory abilities of the transcription factors.

6.0 Literature

1. Avram, D., Fields, A., Top, K. P. O., Nevrivy, D. J., Ishmael, J. E., & Leid, M. (2000). Isolation of a novel family of C2H2 zinc finger proteins implicated in transcriptional repression mediated by chicken ovalbumin upstream promoter transcription factor (COUP-TF) orphan nuclear receptors. *Journal of Biological Chemistry*, *275*, 10315-10322.

2. Arlotta, P., Molyneaux, B. J., Chen, J., Inoue, J., Kominami, R., & Macklis, J. D. (2005). Neuronal subtype-specific genes that control corticospinal motor neuron development in vivo. *Neuron*, *45*, 207-221.

3. Bejerano, G., Pheasant, M., Makunin, I., Stephen, S., Kent, W. J., Mattick, J. S., & Haussler, D. (2004). Ultraconserved elements in the human genome. *Science*, *304*, 1321-1325.

4. Britanova, O., de Juan Romero, C., Cheung, A., Kwan, K. Y., Schwark, M., Gyorgy, A., Vogel, T., Akopov, S., Mišo, M., Agoston, D., Šestan, N., Molnár, Z., & Tarabykin V. (2008). Satb2 is a postmitotic determinant for upper-layer neuron specification in the neocortex. *Neuron*, *57*, 378-392.

5. Califano, D., Cho, J. J., Uddin, M. N., Lorentsen, K. J., Yang, Q., Bhandoola, A., Li, H., & Avram, D. (2015). Transcription factor Bcl11b controls identity and function of mature type 2 innate lymphoid cells. *Immunity*, *43*, 354-368.

6. Cánovas, J., Berndt, F. A., Sepúlveda, H., Aguilar, R., Veloso, F. A., Montecino, M., Oliva, C., Maas, J. C., Sierralta, J., & Kukuljan, M. (2015). The Specification of Cortical Subcerebral Projection Neurons Depends on the Direct Repression of TBR1 by CTIP1/BCL11a. *The Journal of Neuroscience*, *35*, 7552-7564.

7. Cooper-Kuhn, C. M., & Kuhn, H. G. (2002). Is it all DNA repair?: methodological considerations for detecting neurogenesis in the adult brain. *Developmental Brain Research*, *134*, 13-21.

8. Fame, R. M., MacDonald, J. L., & Macklis, J. D. (2011). Development, specification, and diversity of callosal projection neurons. *Trends in neurosciences*, *34*, 41-50.

9. Galazo, M. J., Emsley, J. G., & Macklis, J. D. (2016). Corticothalamic Projection Neuron Development beyond Subtype Specification: Fog2 and Intersectional Controls Regulate Intraclass Neuronal Diversity. *Neuron*, *91*, 90-106.

10. Gorski, J. A., Talley, T., Qiu, M., Puelles, L., Rubenstein, J. L., & Jones, K. R. (2002). Cortical excitatory neurons and glia, but not GABAergic neurons, are produced in the Emx1-expressing lineage. *The Journal of neuroscience*, *22*, 6309-6314.

11. Greig, L. C., Woodworth, M. B., Galazo, M. J., Padmanabhan, H., & Macklis, J. D. (2013). Molecular logic of neocortical projection neuron specification, development and diversity. *Nature Reviews Neuroscience*, *14*, 755-769.

12. Greig, L. C., Woodworth, M. B., Greppi, C., & Macklis, J. D. (2016). Ctip1 controls acquisition of sensory area identity and establishment of sensory input fields in the developing neocortex. *Neuron*, *90*, 261-277.

13. Gu, H., Marth, J. D., Orban, P. C., Mossman, H., & Rajewsky, K. (1994). Deletion of DNA polymerase beta gene segment in T cells using cell-type specific gene targeting in mice. *Science*, *269*, 1427.

14. Hevner, R. F., Shi, L., Justice, N., Hsueh, Y. P., Sheng, M., Smiga, S., Bulfone, A., Goffinet, A. M., Campagnoni, A. T., & Rubenstein, J. L. (2001). Tbr1 regulates differentiation of the preplate and layer 6. *Neuron*, *29*, 353-366.

15. Hevner, R. F., Miyashita-Lin, E., & Rubenstein, J. L. (2002). Cortical and thalamic axon pathfinding defects in Tbr1, Gbx2, and Pax6 mutant mice: evidence that cortical and thalamic axons interact and guide each other. *Journal of Comparative Neurology*, *447*, 8-17.

16. Hancarova, M., Simandlova, M., Drabova, J., Mannik, K., Kurg, A., & Sedlacek, Z. (2013). A patient with de novo 0.45 Mb deletion of 2p16. 1: The role of BCL11A, PAPOLG, REL, and FLJ16341 in the 2p15-p16. 1 microdeletion syndrome. *American Journal of Medical Genetics Part A*, *161*, 865-870.

17. John, A., Brylka, H., Wiegreffe, C., Simon, R., Liu, P., Jüttner, R., Crenshaw E.B. 3rd, Luyten, F. P., Jenkings, N. A., Copeland, N. A., Birchmeier, C. & Britsch, S. (2012). Bcl11a is required for neuronal morphogenesis and sensory circuit formation in dorsal spinal cord development. *Development*, *139*, 1831-1841.

18. Kapuscinski, J. (1995). DAPI: a DNA-specific fluorescent probe. *Biotechnic & Histochemistry*, *70*, 220-233.

19. Kaufman, M. H. (1992). The atlas of mouse development. *Elsevier Academic Press*, Heidelberg, London, New York.

20. Kuo, T. Y., Hong, C. J., & Hsueh, Y. P. (2009). Bcl11A/CTIP1 regulates expression of DCC and MAP1b in control of axon branching and dendrite outgrowth. *Molecular and Cellular Neuroscience*, *42*, 195-207.

21. Kwan, K. Y., Lam, M. M., Krsnik, Ž., Kawasawa, Y. I., Lefebvre, V., & Šestan, N. (2008). SOX5 postmitotically regulates migration, postmigratory differentiation, and projections of subplate and deep-layer neocortical neurons. *Proceedings of the National Academy of Sciences, 105*, 16021-16026.

22. Lai, T., Jabaudon, D., Molyneaux, B. J., Azim, E., Arlotta, P., Menezes, J. R., & Macklis, J. D. (2008). SOX5 controls the sequential generation of distinct corticofugal neuron subtypes. *Neuron*, *57*, 232-247.

23. Latchman, D. S. (1997). Transcription factors: an overview. *The international journal of biochemistry & cell biology*, *29*, 1305-1312.

24. Leid, M., Ishmael, J. E., Avram, D., Shepherd, D., Fraulob, V., & Dollé, P. (2004). CTIP1 and CTIP2 are differentially expressed during mouse embryogenesis. *Gene expression patterns*, *4*, 733-739.

25. Leone, D. P., Heavner, W. E., Ferenczi, E. A., Dobreva, G., Huguenard, J. R., Grosschedl, R., & McConnell, S. K. (2014). Satb2 regulates the differentiation of both callosal and subcerebral projection neurons in the developing cerebral cortex. *Cerebral Cortex, 25,* 3406-3410.

26. Li, P., Burke, S., Wang, J., Chen, X., Ortiz, M., Lee, S. C., Lu, D., Campos, L., Goulding, D., Ng, B. L., Dougan, G., Huntly, B., Gottgens, B., Jenkings, N. A., Copeland, N. G., Colucci, F., & Liu, P. (2010). Reprogramming of T cells to natural killer–like cells upon Bcl11b deletion. *Science*, *329*, 85-89.

27. Liu, P., Keller, J. R., Ortiz, M., Tessarollo, L., Rachel, R. A., Nakamura, T., Jenkins, N. A., & Copeland, N. G. (2003). Bcl11a is essential for normal lymphoid development. *Nature immunology*, *4*, 525-532.

28. McKenna, W. L., Betancourt, J., Larkin, K. A., Abrams, B., Guo, C., Rubenstein, J. L., & Chen, B. (2011). Tbr1 and Fezf2 regulate alternate corticofugal neuronal identities during neocortical development. *The Journal of Neuroscience*, *31*, 549-564.

29. Molyneaux, B. J., Arlotta, P., Menezes, J. R., & Macklis, J. D. (2007). Neuronal subtype specification in the cerebral cortex. *Nature reviews neuroscience*, *8*, 427-437.

30. Oishi, K., Aramaki, M., & Nakajima, K. (2016). Mutually repressive interaction between Brn1/2 and Rorb contributes to the establishment of neocortical layer 2/3 and layer 4. *Proceedings of the National Academy of Sciences, 113,* 3371-3374.

31. Paxinos, G., & Keith, F. (2012). Paxinos and Franklin's the Mouse Brain in Stereotaxic Coordinates, 4th Edition. *Academic Press,* London, Oxford, Boston.

32. Rodríguez-Tornos, F. M., Briz, C. G., Weiss, L. A., Sebastián-Serrano, A., Ares, S., Navarrete, M., Frangeul, L., Galazo, M., Jabaudon, D., Esteban, J A., Nieto, M. (2016). Cux1 enables interhemispheric connections of layer II/III Neurons by regulating Kv1-dependent firing. *Neuron*, *89*, 494-506.

33. Roth, M. M., Dahmen, J. C., Muir, D. R., Imhof, F., Martini, F. J., & Hofer, S. B. (2016). Thalamic nuclei convey diverse contextual information to layer 1 of visual cortex. *Nature neuroscience*, *19*, 299-307.

34. Rubio-Garrido, P., Pérez-de-Manzo, F., Porrero, C., Galazo, M. J., & Clascá, F. (2009). Thalamic input to distal apical dendrites in neocortical layer 1 is massive and highly convergent. *Cerebral cortex, 19,* 2380-2395.

35. Saiki, R. K., Scharf, S., Faloona, F., Mullis, K. B., Horn, G. T., Erlich, H. A., & Arnheim, N. (1985). Enzymatic amplification of b-globin genomic sequences and restriction site analysis for diagnosis of sickle cell anemia. *Science*, *230*, 1350-1354.

36. Saito, T., & Nakatsuji, N. (2001). Efficient gene transfer into the embryonic mouse brain using in vivo electroporation. *Developmental biology*, *240*, 237-246.

37. Satterwhite, E., Sonoki, T., Willis, T. G., Harder, L., Nowak, R., Arriola, E. L., Liu, H., Price, H. P., Gesk, S., Steinemann, D., Schlegelberger, B., Oscier, D. G., Siebert, R., Tucker, P. W., & Dyer, M. J. (2001). The BCL11 gene family: involvement of BCL11A in lymphoid malignancies. *Blood*, *98*, 3413-3420.

38. Sauer, B. (1987). Functional expression of the cre-lox site-specific recombination system in the yeast Saccharomyces cerevisiae. *Molecular and cellular biology*, *7*, 2087-2096.

39. Srinivasan, K., Leone, D. P., Bateson, R. K., Dobreva, G., Kohwi, Y., Kohwi-Shigematsu, T., Grosschedl, R., & McConnell, S. K. (2012). A network of genetic repression and derepression specifies projection fates in the developing neocortex. *Proceedings of the National Academy of Sciences*, *109*, 19071-19078.

40. Simon, R., Brylka, H., Schwegler, H., Venkataramanappa, S., Andratschke, J., Wiegreffe, C., Liu, P., Fuchs, E., Jenkins, N.A., Copeland, N.G., Birchmeier, C., & Britsch, S. (2012). A dual function of Bcl11b/Ctip2 in hippocampal neurogenesis. *The EMBO journal*, *31*, 2922-2936.

41. Simon, R., Baumann, L., Fischer, J., Seigfried, F. A., De Bruyckere, E., Liu, P., Jenkins, N. A., Copeland, N. G., Schwegler, H., & Britsch, S. (2016). Structure-function integrity of the adult hippocampus depends on the transcription factor Bcl11b/Ctip2. *Genes, Brain and Behavior*, *15*, 405-419.

42. Tydell, C. C., David-Fung, E. S., Moore, J. E., Rowen, L., Taghon, T., & Rothenberg, E. V. (2007). Molecular dissection of prethymic progenitor entry into the T lymphocyte developmental pathway. *The Journal of Immunology*, *179*, 421-438.

43. Wakabayashi, Y., Watanabe, H., Inoue, J., Takeda, N., Sakata, J., Mishima, Y., Hitomi, J., Yamamoto, T., Utsuyama, M., Niwa, O., Aizawa, S., & Kominami, R. (2003). Bcl11b is required for differentiation and survival of αβ T lymphocytes. *Nature immunology*, *4*, 533-539.

44. Walker, J. A., Oliphant, C. J., Englezakis, A., Yu, Y., Clare, S., Rodewald, H. R., Belz, G., Liu, P., Fallon, P. G., & McKenzie, A. N. (2015). Bcl11b is essential for group 2 innate lymphoid cell development. *The Journal of experimental medicine, 212, 875-882*.

45. Wonders, C. P., & Anderson, S. A. (2006). The origin and specification of cortical interneurons. *Nature Reviews Neuroscience*, *7*, 687-696.

46. Woodworth, M. B., & Greig, L. C., Kriegstein, A. R., & Macklis, J. D. (2012). SnapShot: Cortical Development. *Cell*, *151*, 918-918.

47. Woodworth, M. B., Greig, L. C., Liu, K. X., Ippolito, G. C., Tucker, H. O., & Macklis, J. D. (2016). Ctip1 regulates the balance between specification of distinct projection neuron subtypes in deep cortical layers. *Cell reports*, *15*, 999-1012.

48. Woolsey, T. A., & Van der Loos, H. (1970). The structural organization of layer IV in the somatosensory region (SI) of mouse cerebral cortex: the description of a cortical field composed of discrete cytoarchitectonic units. *Brain research*, *17*, 205-242.

49. Wiegreffe, C., Simon, R., Peschkes, K., Kling, C., Strehle, M., Cheng, J., Srivatsa, S., Liu, P., Jenkins, N. A., Copeland, N. G., Tarabykin, V., & Britsch, S. (2015). Bcl11a (Ctip1) Controls Migration of Cortical Projection Neurons through Regulation of Sema3c. *Neuron*, *87*, 311-325.

II List of figures

Figure 1	**Distinct progenitor populations generate projection neurons in an "inside-out" fashion**	**3**
Figure 2	**Bcl11a deficient neurons fail to migrate correctly**	**5**
Figure 3	**Bcl11b mutants do not manifest a corticospinal tract (CST)**	**6**
Figure 4	**Model of transcription factors directing neuronal projection differentiation**	**7**
Figure 5	**Genotypes used in this thesis**	**18**
Figure 6	**Bcl11a and Bcl11b are efficiently deleted in AB-mutants at P0**	**27**
Figure 7	**AB-mutant neocortices show a major shrinkage in cortical thickness**	**29**
Figure 8	**Fog2, a typical neocortical marker for layer VI corticothalamic projection neurons, is severely reduced in its expression in AB-mutants**	**31**
Figure 9	**The expression of Sox5, a specific marker for neocortical layers V and VI, is decreased in AB-mutants**	**32**
Figure 10	**Tbr1, a typical layer VI marker, is reduced in its deep-layer typical strong expression**	**33**
Figure 11	**Neurogenesis at early stages of AB-mutants is not impaired compared to controls**	**35**
Figure 12	**AB-mutants show slight increase of apoptosis on E12.5 and E13.5, and a massive increase of apoptosis at P0**	**36**
Figure 13	**Over different embryonic stages, Fog2 expression is reduced in AB-mutants**	**38**
Figure 14	**Sox5 expression is reduced severely in developing AB-mutant brains**	**39**
Figure 15	**Strong, deep-layer typical Tbr1 expression does not appear in AB-mutants, instead overall weak expression is retained throughout the neocortex**	**41**
Figure 16	**Bcl11a and Bcl11b are knocked out efficiently in Bcl11a//b$^{flox/flox}$ neurons that have been transfected with Cre and GFP**	**43**
Figure 17	**In AB-mutant neurons, deep-layer specific markers are decreased**	**45**

	on a cell-autonomous level	
Figure 18	**No apparent difference of cleaved caspase 3 signal in control and mutant brains**	**46**
Figure 19	**Alterations of upper-layer markers in brains electroporated with Cre-IRES-GFP**	**48**

III List of tables

Table 1	**Chemicals**	**11**
Table 2	**Solutions**	**12**
Table 3	**Primers**	**14**
Table 4	**Antibodies**	**14**
Table 5	**Other reagents**	**15**
Table 6	**Ingredients of different PCRs**	**20**

IV Acknowledgements

Deleted due to privacy reasons.

V Curriculum vitae

Deleted due to privacy reasons.